



# Exploring the protective effect of Sangggua Drink against type 2 diabetes mellitus in db/db mice using a network pharmacological approach and experimental validation

Yu Cai<sup>a</sup>, Simin Liu<sup>a</sup>, Fei Zeng<sup>a</sup>, Zhiwei Rao<sup>b</sup>, Chunchao Yan<sup>a</sup>, Qichang Xing<sup>a</sup>, Yunzhong Chen<sup>a,\*</sup>

<sup>a</sup> Hubei Provincial Research Center for TCM Health Food Engineering, School of Pharmacy, Hubei University of Chinese Medicine, Wuhan, 430065, China

<sup>b</sup> Central Hospital of Xianning, The First Affiliate Hospital of Hubei University of Science, China

## ARTICLE INFO

### Keywords:

Sangggua drink  
T2DM  
AMPK/Akt  
db/db mice  
Insulin resistance

## ABSTRACT

Sangggua Drink (SGD) is an experienced formula for clinical treatment of type 2 diabetes mellitus (T2DM). Network pharmacology and experiments were combined to explore the potential mechanism of action of SGD on T2DM. The material basis and action mechanism of SGD were investigated to reveal the active components of SGD, potential target prediction was conducted from TargetNet, PharmMapper; Cytoscape was used to construct PPI network and component-target-pathway (C-T-P) network diagram to interpret biological processes and enrich action pathways. 54 compounds and 41 key target proteins were screened, and a total of 98 signaling pathways were obtained. In vivo experiments, the levels of p-AMPK ( $P < 0.01$ ), p-ACC and p-AKT were significantly increased in the mice with SGD intervention compared to the db/db mice, while level of FOXO1 were decreased. The results suggested that SGD might improve insulin resistance and glucose metabolism in T2DM mice by activating the AMPK/Akt signaling pathway.

## 1. Introduction

T2DM is a metabolic syndrome that increasing in prevalence worldwide. According to statistics: 537 million adults suffer from T2DM in 2021 globally. Compared with 2019, the number of T2DM patients increased by 74 million, an increase of 16%. IDF estimates that this number will reach 783 million by 2045, a 46% increase that is more than twice the estimated population growth (20%) over the same period, and that the proportion of adults affected may reach one in eight [1].

The main cause of T2DM is insulin resistance (IR), which causes the cells to have a reduced effect on the action of a unit concentration of insulin. When the body may continue to produce insulin, the cells in the body become resistant to its behaviour. As a result, the cells are unable to deal effectively with insulin resistance, which leads to hyperglycaemia. Chronic hyperglycaemia can lead to a range of complications such as diabetic cardiovascular disease, diabetic nephropathy, diabetic retinopathy and diabetic neuropathy. As a result, diabetes and its complications seriously endanger human health, affect the quality of life of patients, and cause enormous economic pressure on society and families.

China has a long history of medicinal food and homology culture, and its theory first appeared in the Yellow Emperor's Classic of

\* Corresponding author.

E-mail address: [chyzhhucm@126.com](mailto:chyzhhucm@126.com) (Y. Chen).

<https://doi.org/10.1016/j.heliyon.2023.e18026>

Received 16 February 2023; Received in revised form 28 June 2023; Accepted 5 July 2023

Available online 9 July 2023

2405-8440/© 2023 The Authors. Published by Elsevier Ltd. This is an open access article under the CC BY-NC-ND license (<http://creativecommons.org/licenses/by-nc-nd/4.0/>).

**Table 1**  
The database website information.

Database	Website
TCMSP	<a href="http://tcmospw.com/tcmosp.php">http://tcmospw.com/tcmosp.php</a>
YaTCM	<a href="http://cadd.pharmacy.nankai.edu.cn/yatcm/home">http://cadd.pharmacy.nankai.edu.cn/yatcm/home</a>
TCMID	<a href="http://119.3.41.228:8000/tcmid/search/">http://119.3.41.228:8000/tcmid/search/</a>
TargetNet	<a href="http://targetnet.scbdd.com/">http://targetnet.scbdd.com/</a>
Pharmmapper	<a href="http://www.lilab-ecust.cn/pharmmapper/">http://www.lilab-ecust.cn/pharmmapper/</a>
SwissTargetPrediction	<a href="http://swisstargetprediction.ch/">http://swisstargetprediction.ch/</a>
Uniprot	<a href="https://www.uniprot.org/">https://www.uniprot.org/</a>
GeneCards	<a href="https://www.genecards.org/">https://www.genecards.org/</a>
OMIM	<a href="https://www.omim.org">https://www.omim.org</a>
STRING	<a href="https://www.string-db.org/">https://www.string-db.org/</a>
RCSB PDB	<a href="https://www.rcsb.org">https://www.rcsb.org</a>
Disgenet	<a href="https://www.disgenet.org/">https://www.disgenet.org/</a>
Pubchem	<a href="https://pubchem.ncbi.nlm.nih.gov/">https://pubchem.ncbi.nlm.nih.gov/</a>
Swissdock	<a href="http://www.swissdock.ch/">http://www.swissdock.ch/</a>
Metascape	<a href="http://metascape.org/gp/index.html#/main/step1">http://metascape.org/gp/index.html#/main/step1</a>
Omicsbean	<a href="http://www.omicsbean.cn/">http://www.omicsbean.cn/</a>
GO	<a href="http://www.pantherdb.org/">http://www.pantherdb.org/</a>
KEGG	<a href="https://www.kegg.jp/">https://www.kegg.jp/</a>
Cytoscape	<a href="https://cytoscape.org/">https://cytoscape.org/</a>

Internal Medicine. The management system of medicinal food and homology substances in China has been gradually established since the 1980s, and by November 2021, China's medicinal food and homology substances officially entered the stage of legal management, which also marked that the medicinal food and homology substance-related industries in China formally became an indispensable part of the Chinese medicine industry [2]. SGD is a combination of *Folium Mori*, *Fructus Momordicae Charantiae*, *Radix Puerariae Lobatae* and *Rhizoma Dioscorea* made by Professor Li Jiageng of Hubei University of Chinese Medicine, which has the effects of clearing heat and moistening dryness, nourishing yin, nourishing the liver and benefiting the kidney, and has a certain regulatory effect on type 2 diabetes [3–7]. *Folium Mori*, *Fructus Momordicae Charantiae*, *Radix Puerariae Lobatae* and *Rhizoma Dioscorea* are edible and medicinal plants, and their components have been studied in depth: the active ingredients in *Folium Mori* mainly include flavonoids and flavonoid glycosides, polyphenols, polysaccharides, alkaloids, sterols, volatile oils, amino acids and vitamins [8]; *Fructus Momordicae Charantiae* contains proteins, polysaccharides, flavonoids, saponins, triterpenoids, saponins and vitamins [9]. The main chemical constituents of *Radix Puerariae Lobatae* include flavonoids, triterpenoids, saponins, steroids and alkaloids [10]. The main chemical constituents of *Rhizoma Dioscorea* include polysaccharides, amino acids, fatty acids, yamulose compounds, allantoin, trace elements, starch, etc [11]. In recent years, studies have shown that: alkaloids in *Folium Mori* and their derivatives could lower blood glucose by inhibiting glycosidase activity [12]; total flavonoids of *Radix Puerariae Lobatae* could reverse pancreatic  $\beta$ -cell damage, thereby improving insulin resistance and lowering blood glucose [13]; total saponins of *Fructus Momordicae Charantiae* could lower blood glucose by promoting hepatic glycogen synthesis, inhibiting hepatic glycogenolysis and increasing insulin sensitivity through enhanced GLUT4 expression in peripheral tissues [14]. The hypoglycemic mechanism of polysaccharides of *Rhizoma Dioscorea* might be related to its ability to increase serum anti-reactive oxygen species, improve the activity of key enzymes of glucose metabolism, inhibit oxidative stress, improve immune organs and regulate lipid metabolism disorders [15–18]. However, the complex chemical composition of SGD as a food composition has hindered the elucidation of the effects and molecular mechanisms of T2DM.

Network pharmacology is based on the “disease-gene-target-drug” interaction network, and systematically observes the intervention and impact of drugs on the disease network, thus revealing the mystery of drug synergy in the human body. The holistic and systematic nature of this research strategy is similar to the theory of Chinese medicine, which treats diseases from a holistic perspective, and the multi-component, multi-pathway and multi-target synergistic principles of Chinese medicine and its formulas [19].

Network pharmacology is a multidisciplinary field of research that combines computational and experimental approaches to integrate large amounts of information in order to make new discoveries. In the “network target” theory, it is essential to establish a molecular link between the drug/herbal formulation and the disease/Chinese medical evidence, to network the Chinese medical evidence with the pharmacological action of the drug, and to calculate the target with the highest intersection in order to systematically and intuitively predict the possible principles of therapeutic action of Chinese medicine.

In this study, the key compounds and the key target proteins of SGD were analyzed through network pharmacology, the key signaling pathways for its therapeutic effects on T2DM in the database were screened. Further, the effects of SGD on T2DM and the mechanism of action based on AMPK/Ak signaling pathway were analyzed through in vivo experiments in *db/db* mice to provide a basis for the development of SGD. The effects of SGD on fasting blood glucose (FBG), triglycerides, total cholesterol, LDL, HDL, glucose tolerance, insulin tolerance, glycosylated serum protein (GSP), fasting insulin (FINS) and insulin resistance index (HOMA-IR), oxidative stress index, liver glycogen metabolism index were measured in *db/db* mice.

Pathological analysis of liver tissue sections with H.E. staining was performed. The expression of AMPK, Akt, p-Akt, FOXO1 and ACC proteins in the liver tissue was detected by Western blot. This study was conducted to evaluate the anti-diabetic effect of SGD, to explore its molecular mechanism of action and to lay the foundation for further development of SGD as a new preparation for the prevention and treatment of T2DM.

## 2. Materials and methods

### 2.1. Chemicals and reagents

*Radix Puerariae Lobatae*, *Fructus Momordicae Charantiae*, *Folium Mori*, and *Dioscorea oppositifolia* L were provided by Key Laboratory of Traditional Chinese Medicine Resources and Traditional Chinese Medicine Compound, identified by Dr Zhigang Hu, Hubei University of Chinese Medicine. Metformin Hydrochloride Tablets were purchased from Simo-American Shanghai Squibb Pharmaceuticals Ltd.

Antibodies AMPK $\alpha$ , p-AMPK $\alpha$ , ACC, p-ACC, FAS were purchased from Cell Signaling Technology, antibodies SREBP1 was provided from Solarbio, beta-actin polyclonal antibody was provided from Elascience. The secondary antibody of goat-anti-rabbit was obtained from Cell Signaling Technology. The enzyme-linked immunosorbent assay (ELISA) kit was got from Cusabio Biotech Co. Other consumables related to biochemical analysis were purchased from Elascience. Moreover, the database website was shown in Table 1.

### 2.2. The material basis of SGD

This plant extraction was prepared by adapting our previous procedures used by Wang et al., including 60% ethanol extraction, water extraction, n-butanol extraction, and the alkaloid of SGD extraction [20]. Recently, more rapid and simpler tests of the similarity of database and experimental validation have been developed [21]. Therefore, the compounds of SGD were queried from TCMSp, TCMID, and YaTCM databases directly, and oral bioavailability (OB), drug-likeness (DL), and other related drug activity parameters of these compounds were also collected. The active compounds were screened through absorption, distribution, metabolism, and excretion (ADME) screening and Lipinski Rule of Five. It is worth explaining that OB is calculated using the OBioavail 1.1 system, DL is calculated using the Tanimoto coefficient, and parameters include  $OB \geq 30\%$ ,  $DL \geq 0.18$ , Lipinski Rule of Five  $\geq 0.75$  [22–29]. The  $T_{(a,b)}$  index (1) is defined as follows:

$$T_{(a,b)} = \frac{a \cdot b}{\|a\|^2 + \|b\|^2 + a \cdot b} \quad (1)$$

where  $a$  represents the descriptor vector of the compound to be tested,  $b$  represents the database descriptor vector of drug or drug-like compound. In this study, the  $T_{(a,b)} \geq 0.18$  is selected for the drug-like compounds.

### 2.3. Pivotal targets screening

The potential targets of active components were predicted from Targetnet, PharmMapper, and SwissTargets databases, the parameter conditions for selecting potential targets of the compound are PharmMapper Z-score score  $\geq 0.8$ , Swiss probability  $\geq 0.7$ , Targetnet prediction probability  $\geq 0.5$  [1,30–32]. The T2DM related targets were obtained through DisGeNET, GeneCards, and OMIM databases [33,34]. Finally, the targets of active compounds and the targets of T2DM were merged. For compound  $a$  against target  $b$  in PharmMapper, the Z-score (2) was calculated as follows:

$$Z_{ab} = \frac{F_{ab} - \bar{F}_a}{SD_{F_a}} \quad (2)$$

$$\bar{F}_a = \frac{\sum_{i=1, N_a} F_{ab}}{N_a} \quad (3)$$

$$SD_{F_a} = \sqrt{\frac{\sum_{i=1, N_a} (F_{ab} - \bar{F}_a)^2}{N_a - 1}} \quad (4)$$

where  $F_{ab}$  is the original fit score of ligand  $a$  to pharmacophore target  $b$ .  $\bar{F}_a$  (3) is the average of the fit scores of ligand  $a$  to all targets.  $SD_{F_a}$  (4) is the standard deviation of the  $F_{ab}$  distribution.

### 2.4. Crucial targets analysis and network construction

The analysis of essential targets was performed by using STRING, Metascape, Omicsbean databases, including Gene Ontology (GO) analysis and Kyoto Encyclopedia of Genes and Genomes (KEGG) analysis. The protein-protein interaction (PPI) network, component-target-pathway (C-T-P) network, and other networks were completed through Cytoscape software [35,36].

### 2.5. Animal experiment design

Six-week-old C57BLKS/Leprdb male (db/db) mice and wild-type C57BLKS male (db/m) mice were provided by Nanjing Biomedical Research Institute of Nanjing University. All mice were fed with the standard diet in the SPF environment with the 12-h day and night

**Table 2**  
The compendious compositions of SGD.

No.	Name	Formula	MW	OB (%)	DL	Lipinski Rule of Five	Source
M01	formononetin	C16H12O4	268.28	69.67	0.21	1.00	<i>Radix Puerariae</i>
M02	3'-Methoxydaidzein	C16H12O5	284.28	48.57	0.24	1.00	<i>Radix Puerariae</i>
M03	beta-sitosterol	C29H50O	414.79	36.91	0.75	0.75	<i>Radix Puerariae and Mori Follum</i>
M04	Daidzein	C15H10O4	254.25	19.44	0.19	1.00	<i>Radix Puerariae</i>
M05	puerarin	C21H20O9	416.41	24.03	0.69	0.75	<i>Radix Puerariae</i>
M06	alpha-aminobutyric acid	C4H9NO2	103.14	68.78	0.01	1.00	<i>Balsam Pear</i>
M07	d-galacturonic acid	C6H10O7	194.14	29.75	0.04	0.75	<i>Balsam Pear</i>
M08	galanal a	C20H30O3	318.45	N/A	0.41	1.00	<i>Balsam Pear</i>
M09	momordic acid	C30H46O4	470.76	36.36	0.75	0.75	<i>Balsam Pear</i>
M10	stigmasta-5,22-dien-3-one	C29H48O	412.69	43.83	0.76	0.75	<i>Balsam Pear</i>
M11	vignafuran	C16H14O4	270.28	N/A	0.28	1.00	<i>Balsam Pear</i>
M12	poriferast-5-en-3beta-ol	C29H50O	414.79	36.91	0.75	0.75	<i>Mori Follum</i>
M13	scopolin	C16H20O9	354.34	56.45	0.39	1.00	<i>Mori Follum</i>
M14	Inophyllum E	C25H22O5	402.47	38.81	0.85	0.75	<i>Mori Follum</i>
M15	26-Hydroxy-dammara-20,24-dien-3-one	C30H48O2	440.78	44.41	0.79	0.75	<i>Mori Follum</i>
M16	Isoramanone	C21H32O4	348.53	39.97	0.51	1.00	<i>Mori Follum</i>
M17	Moracin B	C16H14O5	286.30	55.85	0.23	1.00	<i>Mori Follum</i>
M18	Moracin C	C19H18O4	310.37	82.13	0.29	1.00	<i>Mori Follum</i>
M19	Moracin D	C19H16O4	308.35	60.93	0.38	1.00	<i>Mori Follum</i>
M20	Moracin E	C19H16O4	308.35	56.08	0.38	1.00	<i>Mori Follum</i>
M21	Moracin F	C16H14O5	286.30	53.81	0.23	1.00	<i>Mori Follum</i>
M22	Moracin G	C19H16O4	308.35	75.78	0.42	1.00	<i>Mori Follum</i>
M23	Moracin H	C20H18O5	338.38	74.35	0.51	1.00	<i>Mori Follum</i>
M24	4-Prenylresveratrol	C19H20O3	296.39	40.54	0.21	1.00	<i>Mori Follum</i>
M25	Oxysanguinarine	C20H13NO5	347.34	46.97	0.87	1.00	<i>Mori Follum</i>
M26	quercetin	C15H9O7	302.25	46.43	0.28	0.75	<i>Mori Follum</i>
M27	kaempferol	C15H10O6	286.24	41.88	0.24	1.00	<i>Mori Follum</i>
M28	Stigmasterol	C29H48O	412.69	43.83	0.76	0.75	<i>Mori Follum and Rhizoma Dioscoreae</i>
M29	arachidonic acid	C20H32O2	304.47	45.57	0.20	0.75	<i>Mori Follum</i>
M30	Supraene	C30H50	410.72	33.55	0.42	0.75	<i>Mori Follum</i>
M31	Iristectorigenin A	C17H14O7	330.29	63.36	0.34	1.00	<i>Mori Follum</i>
M32	icosa-11,14,17-trienoic acid methyl ester	C26H31O2	320.51	44.81	0.23	0.75	<i>Mori Follum</i>
M33	Norartocarpetin	C15H10O6	286.24	54.93	0.24	1.00	<i>Mori Follum</i>
M34	Linolenic acid ethyl ester	C20H34O2	306.48	46.10	0.20	0.75	<i>Mori Follum</i>
M35	Tetramethoxyluteolin	C19H18O6	342.34	43.68	0.37	1.00	<i>Mori Follum</i>
M36	Skimmin (8Cl)	C15H16O8	324.28	38.35	0.32	1.00	<i>Mori Follum</i>
M37	piperlonguminine	C16H19NO3	273.36	30.71	0.18	1.00	<i>Rhizoma Dioscoreae</i>
M38	Methylcimicifugoside	C38H56O11	688.94	46.31	0.09	0.50	<i>Rhizoma Dioscoreae</i>
M39	dioscoreside c	C52H84O22	1061.36	10.32	0.03	0.25	<i>Rhizoma Dioscoreae</i>
M40	Dioscoreside C qt	C28H44O4	444.72	36.38	0.87	0.75	<i>Rhizoma Dioscoreae</i>
M41	campesterol	C28H48O	400.76	37.58	0.71	0.75	<i>Rhizoma Dioscoreae</i>
M42	24-methylcholest-5-enyl-3beta-O-glucopyranoside	C34H58O6	562.92	20.49	0.67	0.50	<i>Rhizoma Dioscoreae</i>
M43	CLR	C27H46O	386.73	37.87	0.68	0.75	<i>Rhizoma Dioscoreae</i>
M44	Isofucosterol	C29H48O	412.77	43.78	0.76	0.75	<i>Rhizoma Dioscoreae</i>
M45	AIDS180907	C23H22O6	394.45	45.33	0.77	1.00	<i>Rhizoma Dioscoreae</i>
M46	Kadsurenone	C21H24O5	356.45	54.72	0.38	1.00	<i>Rhizoma Dioscoreae</i>
M47	hancinone C	C23H28O6	400.51	59.05	0.39	1.00	<i>Rhizoma Dioscoreae</i>
M48	(-)-taxifolin	C15H12O7	304.27	60.51	0.27	0.75	<i>Rhizoma Dioscoreae</i>
M49	Denudatin B	C21H24O5	356.45	61.47	0.38	1.00	<i>Rhizoma Dioscoreae</i>
M50	hancinol	C22H28O5	372.50	64.01	0.37	1.00	<i>Rhizoma Dioscoreae</i>
M51	diosgenin	C27H42O3	414.69	80.88	0.81	0.75	<i>Rhizoma Dioscoreae</i>
M52	Methylcimicifugoside qt	C33H48O7	556.81	31.69	0.21	N/A	<i>Rhizoma Dioscoreae</i>
M53	24-Methylcholest-5-enyl-3beta-O-glucopyranoside qt	C21H47O1	400.76	37.58	0.72	N/A	<i>Rhizoma Dioscoreae</i>
M54	Daidzin	C21H20O9	416.41	14.32	0.73	0.75	<i>Radix Puerariae</i>

light, temperature ( $25 \pm 2$  °C), humidity (45–75%), and free access to food and water. The Ethics Committee of Wuhan Myhalic Biotechnology Co. Ltd approved all the experimental procedures.

After 2 weeks of adaptive feeding, the postprandial blood glucose (PBG) of mice was detected, thus dividing db/db and db/m mice into 4 groups according to the PBG, including non-diabetic db/m mice received normal saline (db/m, n = 6) as the normal group, db/db mice received normal saline (db/db, n = 6) as the control group, db/db mice received oral metformin 250 mg/kg (db/db + metformin, n = 6) as positive control group, SGD compound prescription 700 mg/kg group (db/db + SGD high, n = 6).

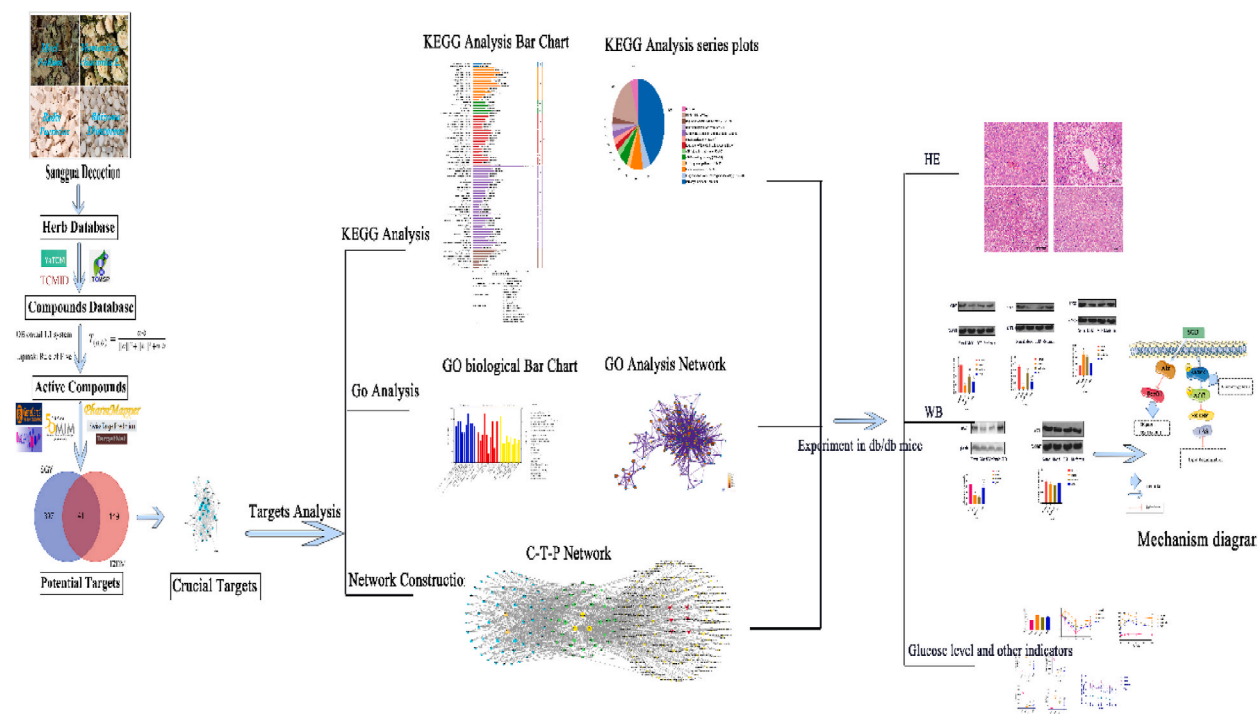


Fig. 1. The flowchart of the study process.

## 2.6. Peritoneal glucose tolerance test

After seven weeks, the intraperitoneal glucose tolerance test (IPGTT) was performed on mice that had been fasted overnight. All mice had been received 1 g/kg glucose in their abdominal cavity. Besides, the intraperitoneal insulin tolerance (IPITT) was performed on mice with a non-fasting state. The mice's blood glucose and insulin level were finally measured at 0, 15, 30, 60, and 120 min.

## 2.7. Serum chemical analysis

All mice fasted for 12 h in week 8, the orbital blood samples were obtained and centrifuged (4°C, 1500×g, 10 min), the glycosylated serum protein (GSP) levels, fasting insulin (FINS), fasting blood glucose (FBG) levels of mice were measured. Homeostasis model assessment (HOMA) was used to assess insulin sensitivity, insulin resistance level and pancreatic  $\beta$  cell function based on the evaluation of epidemiological studies, including HOMA-IR (5), HOMA-IS (6), and HOMA- $\beta$  (7) in detail. The HOMA model is defined as follows:

$$HOMA - IR = \frac{1}{HOMA - IS} = \frac{FBG(\text{mmol/L}) \times FINS (\mu\text{U/mL})}{22.4} \quad (5)$$

$$HOM A - \beta = \frac{20 \times FINS (\mu\text{U/mL})}{[FBG(\text{mmol/L}) - 3.5]} \times 100\% \quad (6)$$

$$HOM A - IS = \frac{1}{[FBG(\text{mmol/L}) * FINS (\mu\text{U/mL})]} \quad (7)$$

## 2.8. Hematoxylin-Eosin (H&E) staining

All the mice were quickly dissected after thoroughly bloodletting. The pancreas, liver tissues and skeletal muscle were cut and separated, rinsed with physiological saline, and fixed in 4% paraformaldehyde solution overnight. The dehydration, embedding, sectioning, staining, and observation, and image capture were finally finished.

## 2.9. Western-blot analysis

After all the mice's tissue samples were sacrificed and collected, the frozen liver, pancreas, and skeletal muscle were sampled in RIPA buffer with protease inhibitors and phosphatase inhibitors. The protein concentration was measured using the BCA protein kit. The protein samples were then separated by 8% SDS-PAGE and were transferred to the polyvinylidene fluoride (PVDF) membrane.

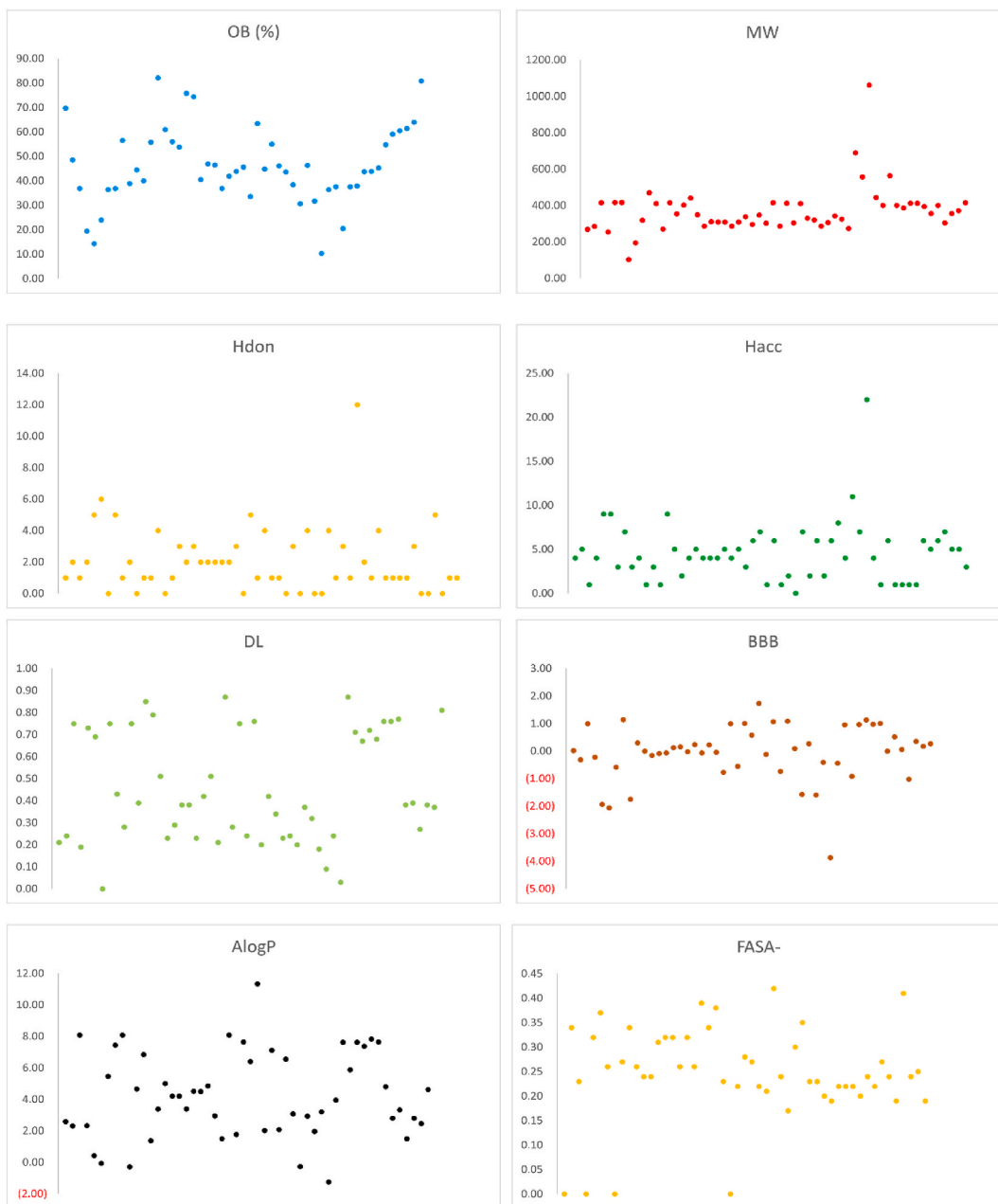
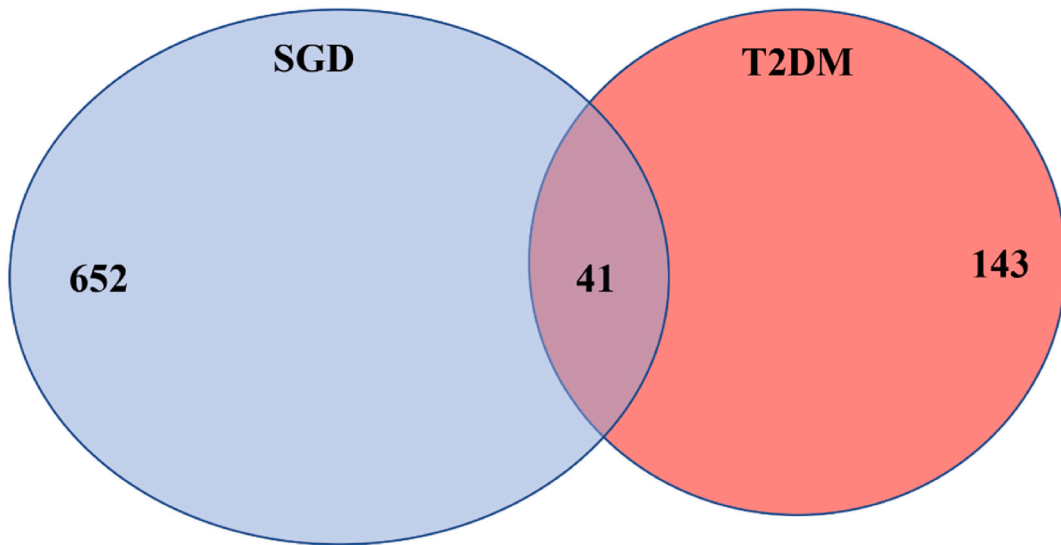


Fig. 2. Scatter diagram of component properties.

After all the samples were blocked with 5% BSA or non-fat dry milk or BSA in TBST, the PVDF membrane was incubated with primary rabbit antibodies against AMPK $\alpha$ , p-AMPK, ACC, p-ACC, FAS, SREBP-1, and  $\beta$ -actin. Then, subsequent procedures were completed one after another, including incubation of secondary antibodies, washing, developing. The protein bands were detected with electrochemiluminescence (ECL) reagent, and the integrated optical density was calculated by Quantit One.

### 2.10. Statistical analysis

All data were analyzed by IBM SPSS Statistics 25.0, the data were expressed as mean  $\pm$  SD, analyzed by ANOVA (One-way analysis of variance), and differences with *p*-value < 0.05 was statistically significant.



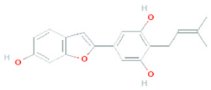
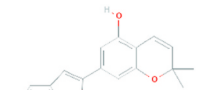
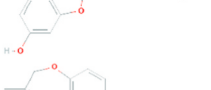
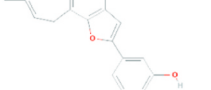
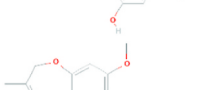
**Fig. 3.** The Venn diagram comparing the composition and disease target genes.

**Table 3**

The information about crucial target proteins.

Number	Target Name	Gene Symbols	Uniprot ID	Degree	Betweenness	Closeness Centrality
1	Serine/threonine-protein kinase AKT	AKT1	P31749	30	0.131	0.800
2	Serum albumin	ALB	P02768	28	0.082	0.769
3	Epidermal growth factor receptor	EGFR	P00533	24	0.065	0.714
4	Mitogen-activated protein kinase 8	MAPK8	P45983	24	0.034	0.714
5	NAD-dependent protein deacetylase sirtuin-1	SIRT1	Q96EB6	23	0.045	0.702
6	Prostaglandin G/H synthase 2	PTGS2	P35354	23	0.086	0.702
7	Peroxisome proliferator-activated receptor gamma	PPARG	P37231	22	0.099	0.690
8	Nitric oxide synthase, endothelial	NOS3	P29474	20	0.025	0.667
9	Matrix metalloproteinase-9	MMP9	P14780	20	0.014	0.667
10	Transcription factor p65	RELA	Q04206	19	0.022	0.656
11	Glucocorticoid receptor	NR3C1	P04150	18	0.032	0.645
12	72 kDa type IV collagenase	MMP2	P08253	18	0.012	0.645
13	Renin	REN	P00797	17	0.027	0.635
14	PI3-kinase p85-alpha subunit	PIK3R1	P27986	15	0.035	0.588
15	Interleukin-2	IL2	P60568	15	0.007	0.606
16	Angiotensin-converting enzyme	ACE	P12821	15	0.011	0.615
17	Insulin-like growth factor 1 receptor	IGF1R	P08069	13	0.012	0.580
18	Nitric oxide synthase, inducible	NOS2	P35228	13	0.008	0.580
19	Tyrosine-protein phosphatase non-receptor type 1	PTPN1	P18031	12	0.004	0.588
20	RAC-beta serine/threonine-protein kinase	AKT2	P31751	12	0.003	0.580
21	Prothrombin	F2	P00734	12	0.017	0.571
22	Dipeptidyl peptidase 4	DPP4	P27487	12	0.026	0.571
23	Histone deacetylase 1	HDAC1	Q13547	11	0.006	0.563
24	Hepatocyte nuclear factor 4-alpha	HNF4A	P41235	11	0.002	0.548
25	Bile acid receptor	NR1H4	Q96R11	8	0.001	0.526
26	Peroxisome proliferator-activated receptor gamma	PPARA	P37231	8	0.001	0.526
27	Mitogen-activated protein kinase 10	MAPK10	P53779	8	0.000	0.533
28	Mineralocorticoid receptor	NR3C2	P08235	7	0.005	0.506
29	Fibroblast growth factor receptor 1	FGFR1	P11362	6	0.000	0.506
30	Prostaglandin G/H synthase 1	PTGS1	P23219	5	0.004	0.471
31	Free fatty acid receptor 1	FFAR1	O14842	5	0.006	0.471
32	Sodium/glucose cotransporter 2	SLC5A2	P31639	5	0.000	0.494
33	Proto-oncogene tyrosine-protein kinase receptor Ret	RET	P07949	4	0.000	0.482
34	Sodium/glucose cotransporter 1	SLC5A1	P13866	4	0.002	0.460
35	Peroxisome proliferator-activated receptor delta	PPARD	Q03181	4	0.000	0.460
36	Fibroblast growth factor receptor 2	FGFR2	P21802	3	0.000	0.476
37	Corticosteroid 11-beta-dehydrogenase isozyme 1	HSD11B1	P28845	3	0.000	0.449
38	Hydroxycarboxylic acid receptor 2	HCAR2	Q8TDS4	3	0.005	0.476
39	Thromboxane-A synthase	TBXAS1	P24557	2	0.000	0.421
40	Melatonin receptor type 1B	MTNR1B	P49286	2	0.001	0.426
41	D (1A) dopamine receptor	DRD1	P21728	2	0.000	0.460

**Table 4**  
Potency and mechanism of active compounds.

Name	Structural	Effectiveness	Pharmacological mechanism	Reference
Moracin C		Reducing postprandial blood glucose	Significantly inhibiting $\alpha$ -glucosidase and tyrosinase	[37]
Moracin D				
Moracin G				
Moracin H				
Norartocarpetin		Reducing postprandial hyperglycemia; regulating glucose metabolism	Inhibiting $\alpha$ -glucosidase activity; promoting islet $\beta$ -cell repair; inhibiting non-enzymatic protein glycosylation; regulating the expression of JNK, IRS-1, Akt-1, PDX-1 mRNA genes in the JNK signaling pathway.	[38,39]

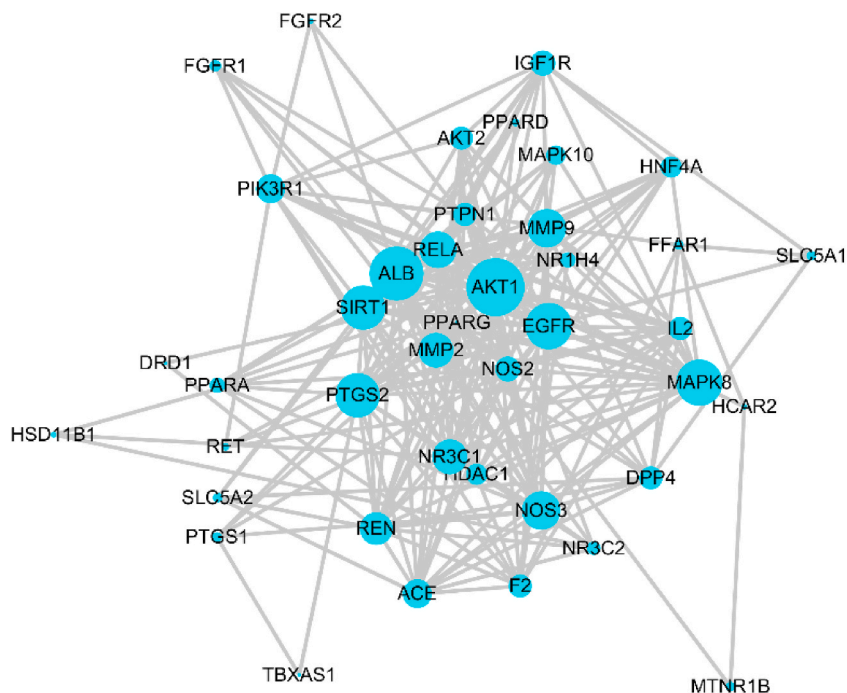


**Fig. 4.** Protein–protein interaction network of SGD acting on T2DM.



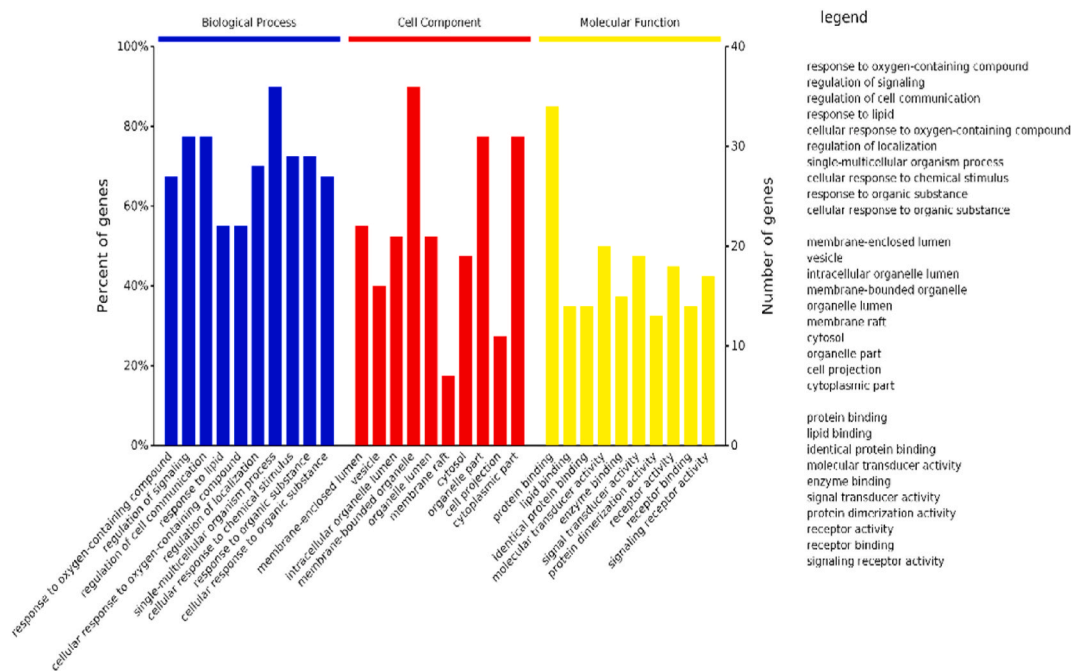


Fig. 5. GO biological Bar Chart.

### 3. Results

#### 3.1. Network pharmacology

Traditional Chinese medicine (TCM) includes complex formulations that are difficult to quantify accurately, thus limiting its wide clinical application. Here we screened the active ingredients in the drug composition of SangGua Drink (SGD) formula to obtain the intersection with diabetic target proteins, and also analyzed the potential target protein interactions by ppi protein interaction network to obtain the relationship network between active ingredients and diabetic target proteins, and analyzed the key target GO biological process by Cytoscape clue go plug-in and Omicsbean. Finally, Cytoscape (v3.8.2) was used to construct a component-target-pathway (C-T-P) network to illustrate the mechanism of action of SGD components.

##### 3.1.1. Compound identification and potential target analysis of SGD

The active compounds of SGD were screened by the compound database ADME and finally 54 compounds were obtained and listed in Table 2. Dioscoreside C<sub>qt</sub>, Methylcimicifugoside<sub>qt</sub>, etc. The active properties of all active compounds are shown in Fig. 1. They include alkaloids, saponins, flavonoids, polysaccharides, and glycosides formed by glucose water loss (24-Methylcholest-5-enyl-3beta-O-glucopyranoside<sub>qt</sub>, Dioscoreside C<sub>qt</sub>, Methylcimicifugoside<sub>qt</sub>, etc. The active properties of all the compounds are shown in Figs. 2 and 3. Each component of SGD contains multiple active compound components, which act on multiple targets through multiple mechanisms. There are 41 overlapping genes between the active target of the drug and the pathogenic target of T2DM, which may be the key genes involved in the treatment of T2DM by SGD (Table 3). The pharmacological mechanisms of some of the active compounds of SGD are also described below (Table 4).

##### 3.1.2. Analysis of protein interactions and key targets

The PPIprotein interaction network was used to analyze the potential target protein interactions, to construct the relationship for the potential targets and to find the key targets, and finally cytoscape obtained the ppi protein interaction network graph in Fig. 4, where the larger the degree value indicates the greater the importance of the target, containing 42 points and 245 edges of the relationship, and the ppi average node degree is 12.2, the ppi network reveals the interaction relationship of key targets of SGD activity, which is the key target for its pharmacological treatment of T2DM.

##### 3.1.3. GO biological process analysis

By using Cytoscape clue go plug-in and Omicsbean to analyze the key target GO bioprocesses, we finally obtained the GO bioprocess interrelationship network and bioprocess specific bar graphs, as which is shown in Fig. 5. The graphical interpretation of the biological process of SGD for T2DM is divided into Biological Process (Fig. 6), Cell Component (Figs. 7 and 8), and Molecular Function (Figs. 9 and 10), and the three biological processes with the most weight are single-multicellular organism process, The most weighted processes are single-multicellular organism process, membrane-bounded organelle, protein binding, while the GO biological process

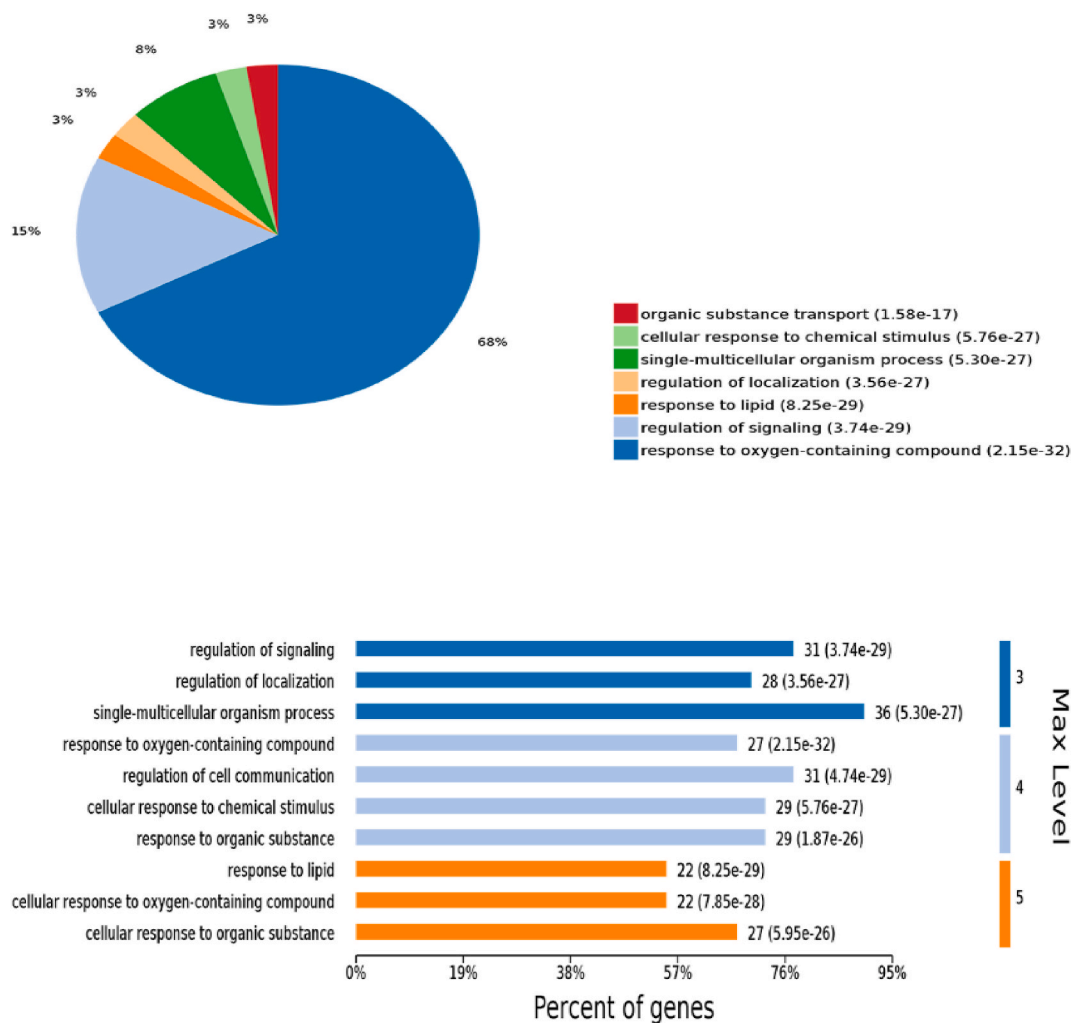


Fig. 6. Biological process.

network relationship diagram (Figs. 11 and 12) reveals the relationship network for specific biological process regulation, among which the more weighted ones are negative regulation of cholesterol storage, glucose transmembrane transport, etc.

### 3.1.4. KEGG pathway analysis

The KEGG pathway analysis of 46 key targets was performed by Omicsbean and Metescape, and a total of 104 signaling pathways were obtained, and the KEGG pathway relationship histogram Figs. 13 and 14 was obtained, which mainly includes Pathway in cancer, AMPK signaling pathway, MAPK signaling pathway, etc. pathway in cancer, AMPK signaling pathway, MAPK signaling pathway, etc. The pathway relationship diagram and the histogram explained the pathway mechanism of SGD for pharmacological treatment of T2DM.

### 3.1.5. Component-target-pathway (C-T-P) network construction

Cytoscape (v3.1.2) was used to construct a component-target-pathway (C-T-P) network relationship diagram, which is shown in Fig. 15 and contains 193 nodes (54 chemical components, 46 key targets, 104 signaling pathways), which reveals the mechanism of action of SGD components.

For compound components, galanal a, poriferast-5-en-3beta-ol are the key components of SGD for T2DM; for targets, AKT1, AKT2, RELA are the key targets of SGD for T2DM; for signaling pathways, Insulin resistance, PI3K/AKT signaling pathway, MAPK signaling pathway, etc. are the key pathways of T2DM treatment by SGD, while AMPK signaling pathway and JAK-STAT signaling pathway are also the key pathways of T2DM treatment by SGD.

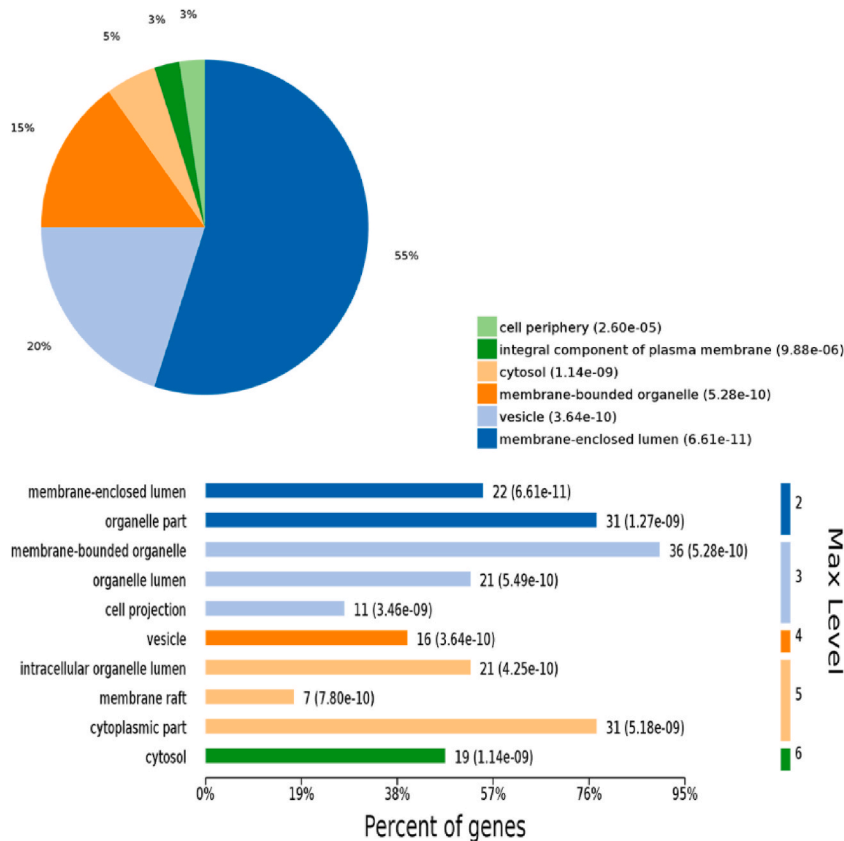


Fig. 7. Cell component.

### 3.2. Animal experiments

#### 3.2.1. Effect of SGD on PBG, FBG, HOMA-IR and HOMA-IS in db/db mice

The postprandial blood glucose (PBG) levels of all mice were shown in Fig. 16. During 10 weeks, there was no significant difference in PBG (Fig. 16) between the SGD group and the Metformin group, and no significant difference in PBG between the SGD and Metformin groups and the Normal group. At week 5, PBG in both metformin and SGD groups were highly significantly different from the model group ( $p < 0.05$ ;  $p < 0.001$ ), while at week 10 both metformin and SGD groups were significantly different from the model group ( $p < 0.05$ ;  $p < 0.01$ ).

HOMA-IR, HOMA-IS models are used to evaluate the level of insulin resistance, the higher the HOMA-IR, the stronger the insulin resistance, the lower the HOMA-IS, the weaker the insulin sensitivity. In this study, as showing in Fig. 17 the levels of HOMA-IR in the SGD mice decreased significantly ( $p < 0.01$ ) and the levels of HOMA-IS increased significantly ( $p < 0.05$ ) compared with those in the Model group, demonstrating the efficacy of SGD on the improvement of insulin resistance.

#### 3.2.2. Effect of SGD on IPGTT and IPITT in db/db mice

The results of the mouse Intraperitoneal Insulin Tolerance Test (IPGTT) and Intraperitoneal Glucose Tolerance Test (IPITT) assay are shown in Figs. 18 and 19.

During 120 min, the IPGTT of both model and control mice were highly significantly different ( $p < 0.01$ ), while the IPGTT of both metformin and SGD groups were not significantly different from that of the Model and Normal groups.

At the 30th minute, there was a significant difference in IPITT between the Model group and the Normal group ( $p < 0.05$ ) and between the SGD group and the model group ( $p < 0.05$ ), while there was no significant difference in IPITT between the SGD group and the control group. At the 60th minute, there was a significant difference in IPITT between the model group and the control group ( $p < 0.05$ ), and a significant difference in IPITT between the SGD group and the model group ( $p < 0.05$ ), while there was no significant difference in IPITT between the SGD group and the control group.

#### 3.2.3. Effects of SGD on GSP, GS, hepatic glycogen, G-6-P, PYGL and GCK levels in db/db mice

A number of studies have proved that Glycated Serum protein (GSP) is a good indicator to reflect the recent control of diabetes and to predict complications [40], so the level of GSP was detected. The GSP level (Fig. 20) of the SGD group was significantly lower than

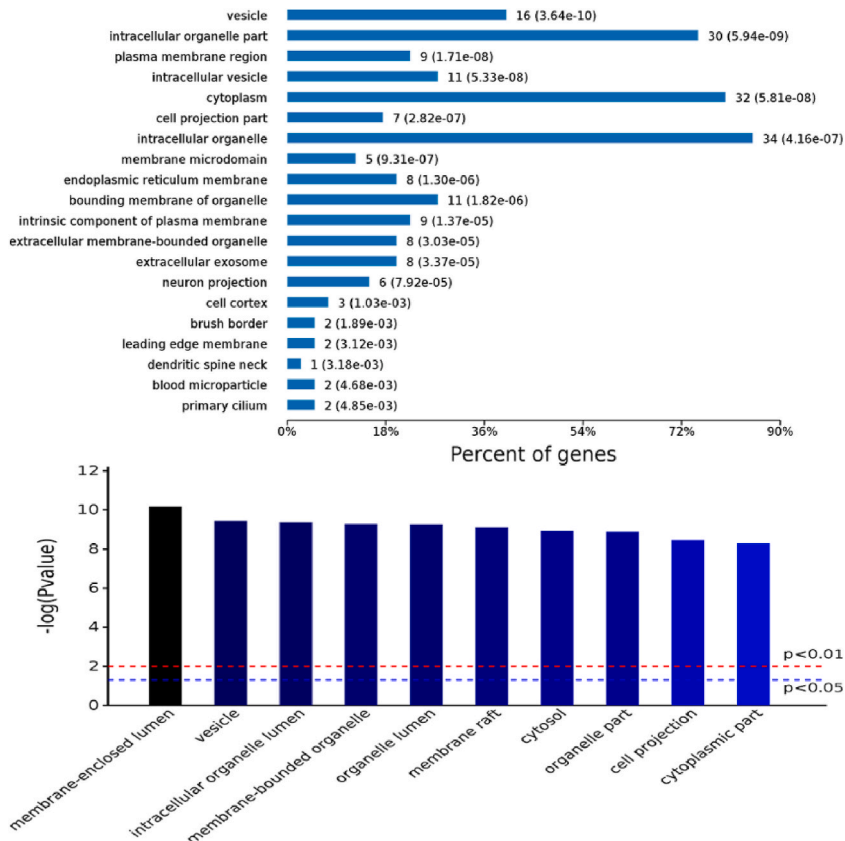


Fig. 8. Cell component.

that of the model group ( $p < 0.05$ ), which proved that SGD could improve the diabetes indicators of db/db mice by reducing the GSP level. At the same time, as shown in Table 5, the levels of liver glycogen, Glycogen Synthase (GS) and glycogen synthase kinase (GCK) in the SGD group were significantly higher than those in the model group ( $p < 0.01$ ), proving that SGD promotes glycogen by promoting AMPK phosphorylation Synthesis of the original, reducing the concentration of free glucose.

3.2.4. Effects of SGD on CAT, GSH-Px, MDA, T-SOD levels in db/db mice

The level of reactive oxygen species (ROS) scavenging was indirectly reflected by measuring the activity of T-SOD, CAT and GSH-Px, the level of lipid peroxidation was reflected by measuring the MDA content, and the level of oxidative stress was directly reflected by measuring the NO content. The results (Table 6) showed that the GSH- Px level in the SGD group was significantly higher than that in the model group ( $p < 0.01$ ), while the MDA content was significantly lower than that in the model group ( $p < 0.01$ ), thus demonstrating that SGD could improve the oxidative stress level in dv/db mice by enhancing the activity of GSH-Px and reducing the MDA content.

3.2.5. Effects of SGD on TG, TC, LDL-C, HDL-C levels in db/db mice

The primary pathophysiological changes of type 2 diabetes mellitus and its complications were lipid metabolism disorders. To assess whether SGD can improve hyperlipidemia, lipid levels in mice were studied. The TG, TC, LDL-C, HDL-C levels of all mice were shown in Table 7. The levels of HDL-C, LDL-C, TC, and TG in the model group were highly significantly different from those in the normal group ( $p < 0.05$ ;  $p < 0.01$ ) The levels of TC, TG, and LDL-C in the SGD group were highly significantly different from those in the model group ( $p < 0.05$ ;  $p < 0.01$ ).

3.2.6. Morphological effects of SGD on the liver of db/db mice

Numerous studies have shown that lipid accumulation in liver tissue correlates with type 2 diabetes, and as one of the main target organs for insulin action, the liver is an important site for glucolipid metabolism in the body. Under the stimulation of long-term high-fat and high-sugar, the liver metabolic function is impaired and the morphological structure is damaged to some extent.

The experimental results showed in Fig. 21 that the hepatocytes in the normal control group had regular morphology, the nucleus was located in the center of the cell, the cell morphology was normal, the arrangement was regular, the tissue structure was intact and clear, and there were no obvious pathological changes; a large number of liver cells in the model control group showed edema,

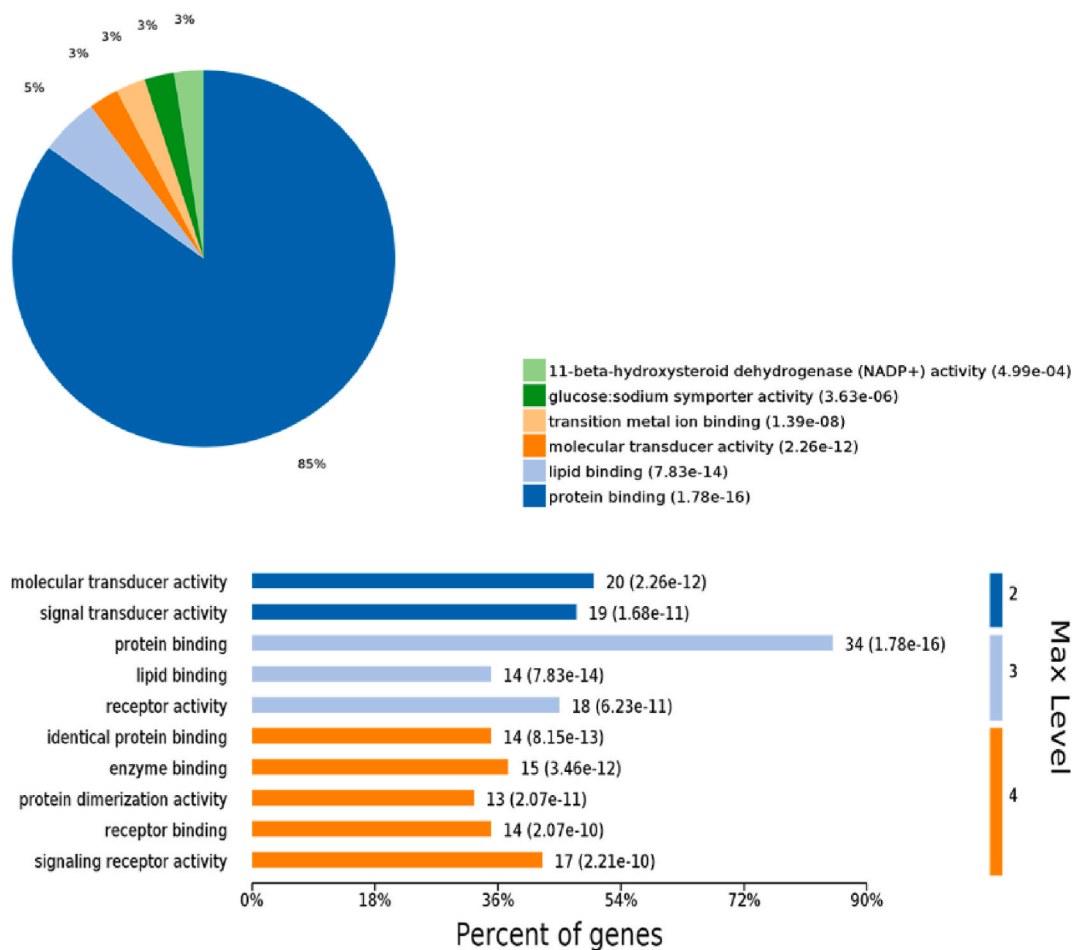


Fig. 9. Molecular function.

disorganized tissue structure and irregular arrangement; the hepatocytes in the metformin group showed edema and necrosis and disorganized cell arrangement; while the hepatocytes in the mulberry gourd drink group had normal morphology, arrangement and tissue structure and no obvious pathological changes.

### 3.2.7. Effects of SGD on the expression of ACC, AMPK, FOXO1, AKT, p-AKT in the liver of db/db mice

FoxO1 is a transcriptional factor encoding genes for gluconeogenesis and its transcriptional activity is downregulated by phosphorylation of Akt. Therefore the levels of FOXO1 and Akt were examined to investigate whether SGD activates this pathway. The results in Fig. 22 showed that there was no significant difference in the expression level of AKT (A) between the four groups, but the level of FOXO1 (E) in the SGD group was significantly lower than that in the normal group ( $P < 0.05$ ). Meanwhile, p-AKT (D) expression in the SGD group was highly significantly different from that in the model group ( $P < 0.01$ ), while the ability of SGD to elevate p-AKT levels was lower than metformin ( $P < 0.05$ ). Phosphorylated AMPK induces free glucose glycogenization and also indirectly promotes avoidance of lipid accumulation by promoting ACC phosphorylation expression, so we examined the level of p-ACC, and the results showed that ACC (B) expression in the SGD group was significantly different from the model group ( $P < 0.05$ ) and from the metformin group ( $P < 0.05$ ). It was demonstrated that the levels of AMPK (C) were significantly degraded in Model group and SGD group compared to Normal group ( $P < 0.01$ ), while the level in SGD group was increased than Model group. The signaling pathways affected by SGD are shown in Fig. 23.

The levels of AMPK, ACC, FOXO1, Akt, p-Akt were measured by protein blotting and the values were expressed as mean  $\pm$  SD ( $n = 6$ ).

## 4. Discussion

### 4.1. Network pharmacology analysis in SGD

Network Pharmacology (NP) research provides additional insights into the overall interactions between therapeutic targets and the

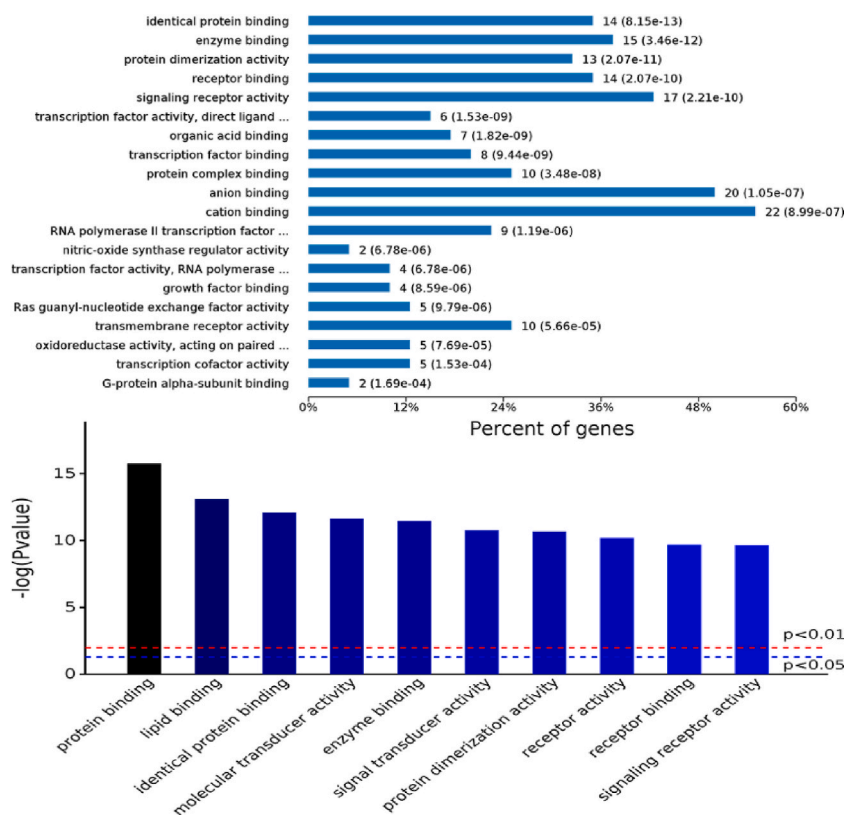


Fig. 10. Molecular function.

disease itself. It is a highly promising and robust technique for illuminating disease processes and discovering possible bioactive components at a collective level.

Pathway compound target (PCT) network revealed that 46 T2DM genes were linked to 41 chemicals (out of 54 chemicals) and 104 pathways in the diagnostic mechanism of T2DM.

For compound components, Galanal A, poriferast-5-en-3beta-ol are the key components of SGD for T2DM; for targets, AKT1, AKT2, RELA are the key targets of SGD for T2DM; for signaling pathways, Insulin resistance, PI3K/AKT signaling pathway, MAPK signaling pathway, etc. are the key pathways of T2DM treatment by SGD, while AMPK signaling pathway and JAK-STAT signaling pathway are also the key pathways of T2DM treatment by SGD. AMPK/Akt signaling pathway: Protein expression of ACC may be the potential therapeutic candidates against T2DM of SGD.

GO analysis described the genes and their products of SGD herbs in terms of biological processes, molecular functions and cellular components, showing that SGD affects human body mainly from two significant processes: single-multicellular biological processes, and protein binding, and the gene products of SGD are mainly concentrated in membrane-bound organelles.

KEGG analysis shows that insight into the specific metabolic pathways involved in SGD active ingredients, of which the Akt signaling pathway and AMPK signaling pathway are presumed to be key signaling pathways.

A network pharmacology of *Phyllanthus emblica* L. fruit (PEf) showed that there are 183 active Pef target genes that act on T2DM, and a PPI network map showed that each gene interacts with its neighbours by creating 183 nodes connected by 1478 edges and by a compound-target disease network. The PPI network showed that each gene interacted with its neighbours by creating 183 nodes connected by 1478 edges, and that quercetin was the most potent compound in Pef targeting T2DM through the compound-target network [41]; A network pharmacology study on *Sorghum bicolor* (SB) showed that the therapeutic effect of SB on T2DM was associated with 16 of the 20 compounds detected by GC-MS, with 118 active target genes acting on T2DM [42].

#### 4.2. Discussion on db/db model mice

Db/db mice is a kind of congenital type 2 diabetes mice caused by Leptin receptor gene defect. This kind of mice was first discovered by Bar Harbor in the inbred line C57BLKS/J (BKS) in 1966. Because its phenotype of hyperglycemia, polyuria and high urine sugar level is similar to that of human diabetes patients, it is called db/db mouse [43]. This mouse is at the age of 2–3 months, although the insulin level is 6–10 times that of normal, the blood glucose level can reach 22–33 mmol·L<sup>-1</sup>, which is an ideal animal model of type 2 diabetes. This mouse has been designated by FDA as one of the spontaneous animal models for studying the application of type 2 diabetes drugs.

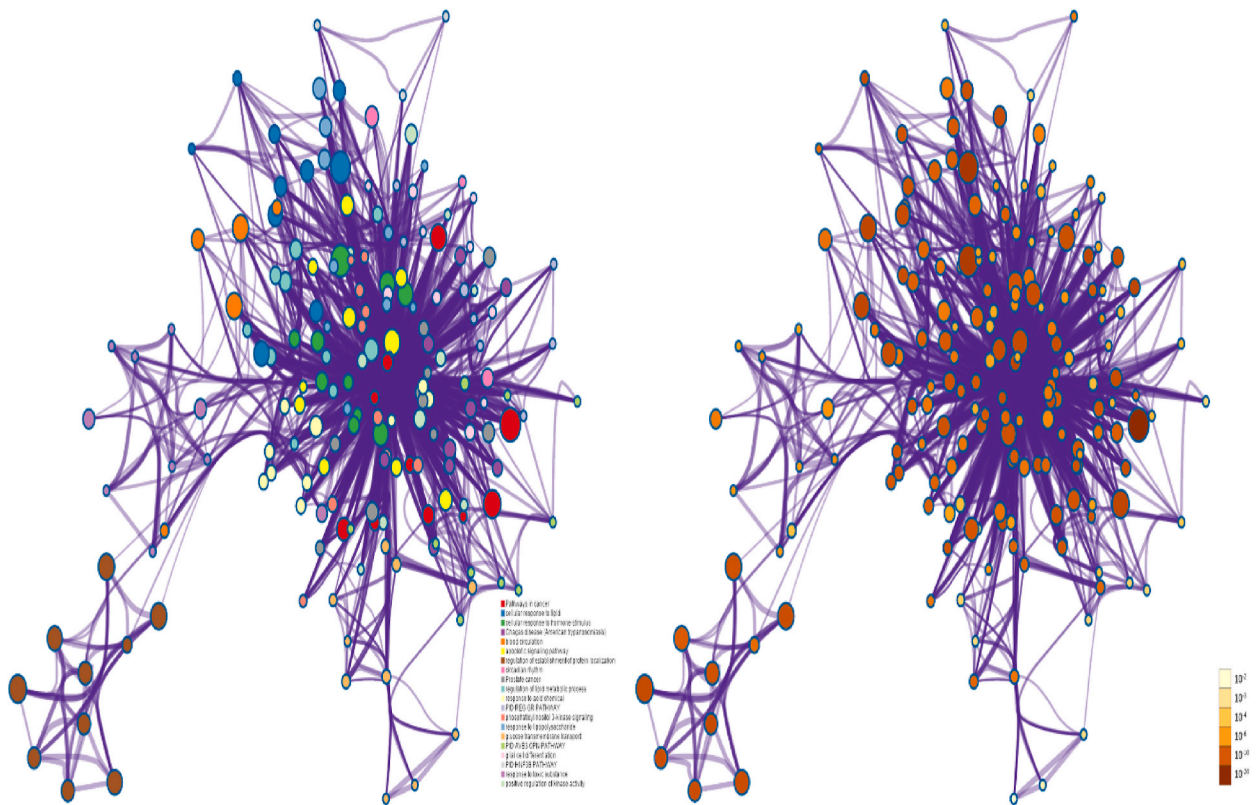


**Fig. 11.** The interaction network of the Gene Ontology (GO) biological enrichment analysis.

#### 4.3. Effect of SGD on food intake, water consumption and body weight in db/db mice

One of the distinctive features of diabetes mellitus is excessive drinking, excessive eating and wasting, while the dietary and water consumption and body weight values of the four groups of mice demonstrated that the body weight of the mod group was significantly lower and the dietary and water consumption was higher, while the body weight of the mice in the SGD group was higher than that of the mice in the Model group and the dietary and water consumption was also lower, approaching the level of the normal group.

#### 4.4. Effect of SGD on FBG level in db/db mice

Insulin is the only protein hormone secreted by pancreatic  $\beta$ -cells that could lower blood glucose in the body, and it can control blood glucose homeostasis and participate in glucose metabolism regulation [44]. Fasting serum insulin could be used as a basic indicator of pancreatic function and insulin resistance in the body. Insulin resistance is a state in which the cellular effect of insulin per unit concentration is diminished and the normal dose of insulin is lower than its biological effect. In this study, FBG, HOMA-IR and of type 2 diabetic mice were significantly increased, HOMA-IS was significantly reduced, suggesting that insulin resistance exists in type 2 diabetic model mice, and the sensitivity and responsiveness of surrounding target tissues to insulin is reduced, which affects the absorption and utilization of glucose by insulin target tissues, resulting in increased compensatory insulin secretion and elevated blood glucose, which is consistent with literature reports. In contrast, the levels of HOMA-IR was significantly reduced after using SGD or metformin. Meanwhile, HOMA-IS levels were significantly higher in SGD group and Metformin group compared to Model group ( $P < 0.05$ ), and there was no significant difference in HOMA-IS and HOMA-IR levels between the two groups. It indicates that SGD could improve insulin resistance in mice with type 2 diabetes mellitus model.

#### 4.5. Effect of SGD on PBG level in db/db mice

In this experiment, compared with the Normal group, the PBG levels of the diabetic model mice increased significantly within 10 weeks, and the PBG levels of the Model group mice without medication reached the lowest peak at week 3, while the PBG levels of the mice receiving SGD and Metformin gradually decreased and reached the lowest values at week 7 (Metformin) and 8 (SGD), respectively, and then fluctuated upward, demonstrating that SGD can effectively reduce blood glucose levels.

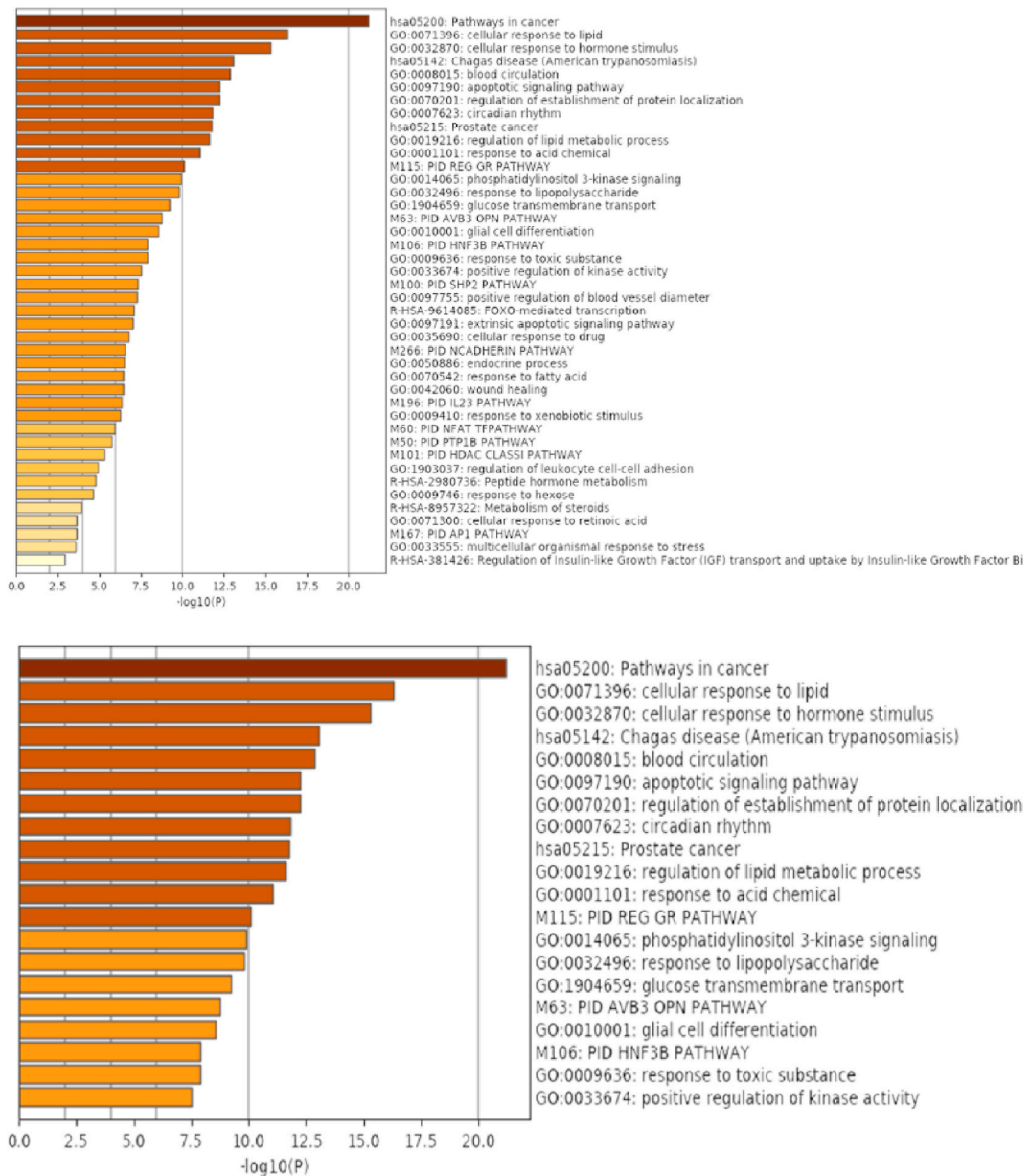


Fig. 12. The GO correlation heat map.

4.6. Effect of SGD on IPGTT and IPITT levels in db/db mice

One of the important aspects in the pathogenesis of type 2 diabetes is reduced glucose tolerance. When the body develops insulin resistance, insulin target tissues become less sensitive to insulin, and peripheral tissues such as liver, fat and skeletal muscle have a reduced ability to take up, convert and utilize glucose, resulting in increased blood glucose levels, which manifest as impaired glucose tolerance.

In the study, compared with normal control mice, the levels of IPGTT and IPITT were significantly higher ( $p < 0.01$ ), while their levels were significantly lower after treatment with metformin and SGD, indicating that SGD improved glucose tolerance and insulin tolerance in db/db mice. The mean value of IPITT level in SGD group was significantly lower than that in Model group, while Metformin group was not significantly different from Model group.

4.7. Effect of SGD on HDL-C, LDL-C, TC, and TG levels in db/db mice

Lipid metabolism disorders could affect insulin resistance and its secretion defects, which are the main causes of diabetes. In 2001,



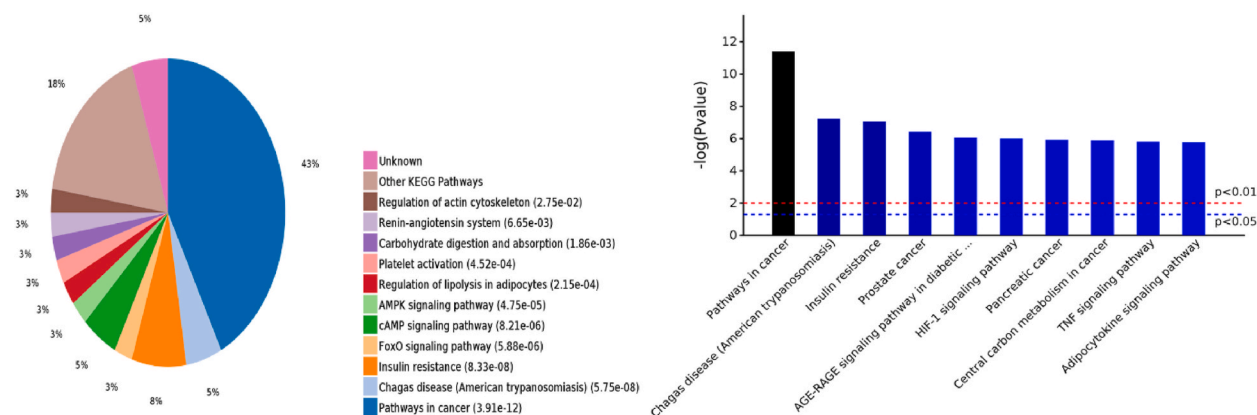


Fig. 13. The KEGG series plots; The KEGG statistical sectoral chart.

McGarry proposed to name type 2 diabetes mellitus “glucolipid disease”, believing that the primary pathophysiological changes of type 2 diabetes mellitus and its complications were lipid metabolism disorders, and the lipid metabolism disorders were the fundamental causes of glucose metabolism disorders, reflecting the importance of lipid metabolism disorders in the pathogenesis of type 2 diabetes mellitus [45]. Increased blood lipids could cause vascular damage, of which atherosclerosis is the most significant, especially the damage to the heart, brain, kidney and other vital tissues and organs’ blood vessels, which would lead to the occurrence of large vascular complications such as diabetic cardiovascular and diabetic cerebrovascular diseases. Therefore, reducing blood lipid contributes to enhancing the glucose uptake by peripheral tissues, improving the function of pancreatic  $\beta$ -cells and insulin activity, reducing insulin resistance, and preventing and treating diabetes and its complications.

In this study, the levels of HDL-C, LDL-C, TC, and TG were significantly increased in diabetic mice. After metformin and SGD administration, the levels of LDL-C, TC, and TG were significantly decreased ( $P < 0.0002$ ) compared with those of the unmedicated Model group mice, but the levels of HDL-C were significantly increased and were extremely significantly higher than those of the Normal group. The classical function of HDL is to mobilize cholesterol from extrahepatic tissues for transport to the liver for excretion, so higher HDL-C levels are beneficial for cardiovascular health. However, it has also been shown that very high HDL-C levels may also have a negative effect on cardiovascular health [46].

#### 4.8. Effect of SGD on SOD, CAT, GSH-Px and MDA levels in db/db mice

The oxidative stress indexes SOD, CAT, GSH-Px and MDA in the serum of mice in each group were determined: MDA is mainly a metabolite produced by oxygen free radicals through oxidation reaction, and its level can reflect the degree of peroxidation and oxidative stress of the body, thus indirectly reflecting the content of oxygen free radicals [47–49]. SOD is the main oxygen free radical scavenging enzyme in the body, which mainly scavenges oxygen free radicals in the body through disproportionation reaction, so the ability to scavenge free radicals is generally evaluated by measuring SOD [47,48,50]. GSH-Px can stabilize cell membrane structure and protect cell function, which is an important part of antioxidant defense system in vivo [45,46,49]; The activity of CAT reflects the ability of organism to scavenge free radicals, which can decompose toxic substances and scavenge free radicals in vivo [51,52].

The experimental results showed that the activities of total superoxide dismutase (T-SOD), catalase (CAT) and glutathione peroxidase (GSH-Px) in model control group db/db mice were significantly decreased, while the content of malondialdehyde (MDA) was significantly increased, indicating that the antioxidant system in vivo was destroyed. Compared with model mice, the antioxidant system in metformin group and SGD group was significantly improved, indicating that SGD could improve the antioxidant capacity of db/db mice in vivo, which might be related to reversing the lesions of liver tissues, and improving the IR effect.

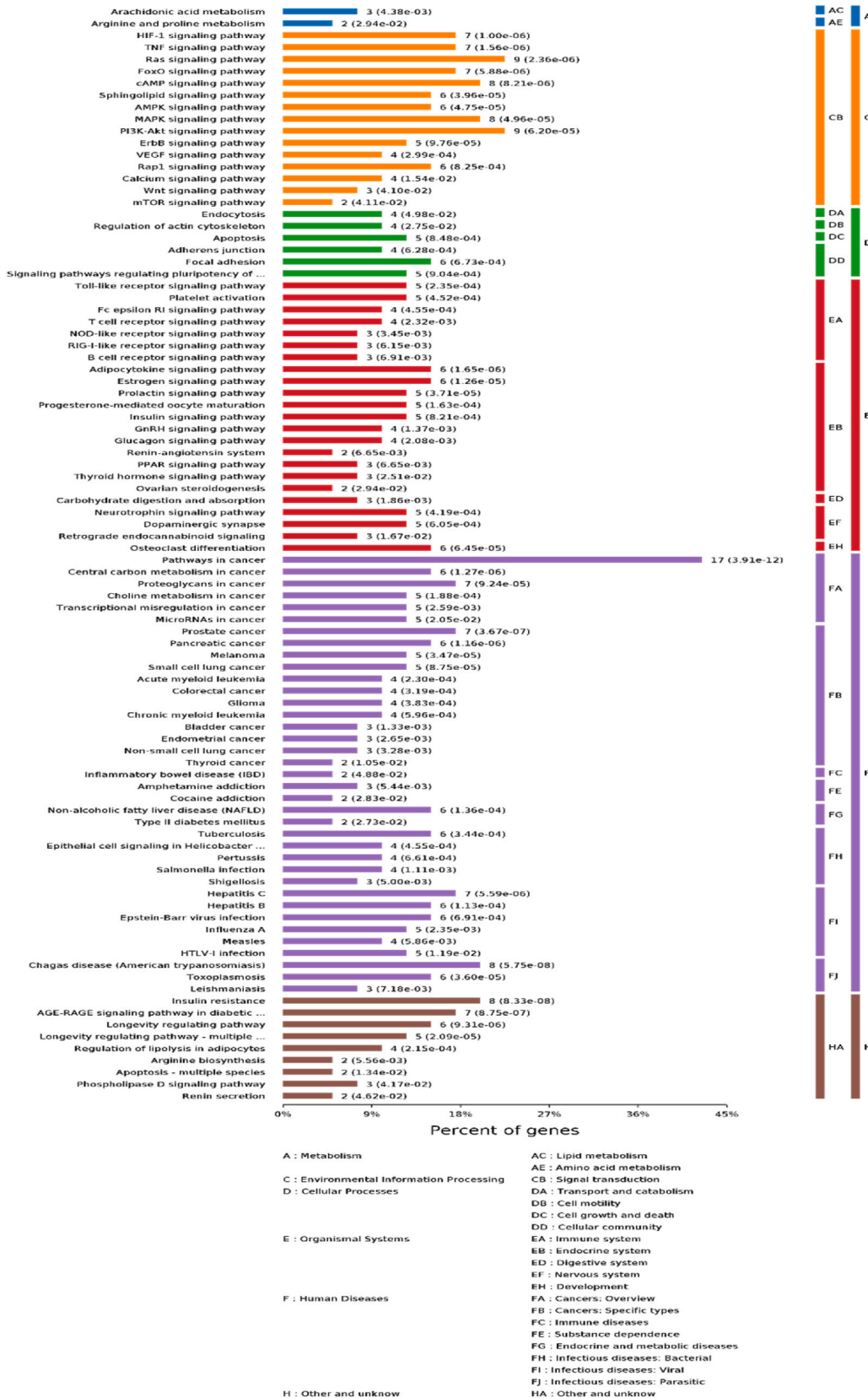
#### 4.9. Effect of SGD on GCK, G-6-P, GP, PYGL and hepatic glycogen levels in db/db mice

Glucokinase (GCK), known as glucose receptor, is involved in various pathways of glucose metabolism. It is mainly distributed in islet  $\beta$  cells and hepatocytes. GCK reduces blood glucose by increasing insulin release and promoting the use of glucose in the liver, playing an important role in maintaining blood glucose homeostasis [53].

In the liver, when the body blood glucose is increased, glucokinase can specifically phosphorylate glucose to produce glucose 6-phosphate, which is synthesized by glycogen synthesis pathway under the action of insulin and stored in liver glycogen. When the blood glucose was decreased, the GCK activity was decreased, and the hepatic glucose output was increased, thereby ensuring the energy supply to important organs.

Glucose -6- phosphatase (G-6-pase) is a phosphatase that hydrolyzes phosphate compounds. Glucose is released into the blood through the hydrolysis of glucose -6- phosphate in the liver tissue, which increases the blood glucose and maintains the balance of blood glucose. It is also one of the key enzymes for liver glucose metabolism.

Glycogen synthase (GS) catalyzes the production of glycogen and UTP from uridine diphosphate glucose (UDPG) and glucose



(caption on next page)

Fig. 14. The KEGG statistical significance bar chart.

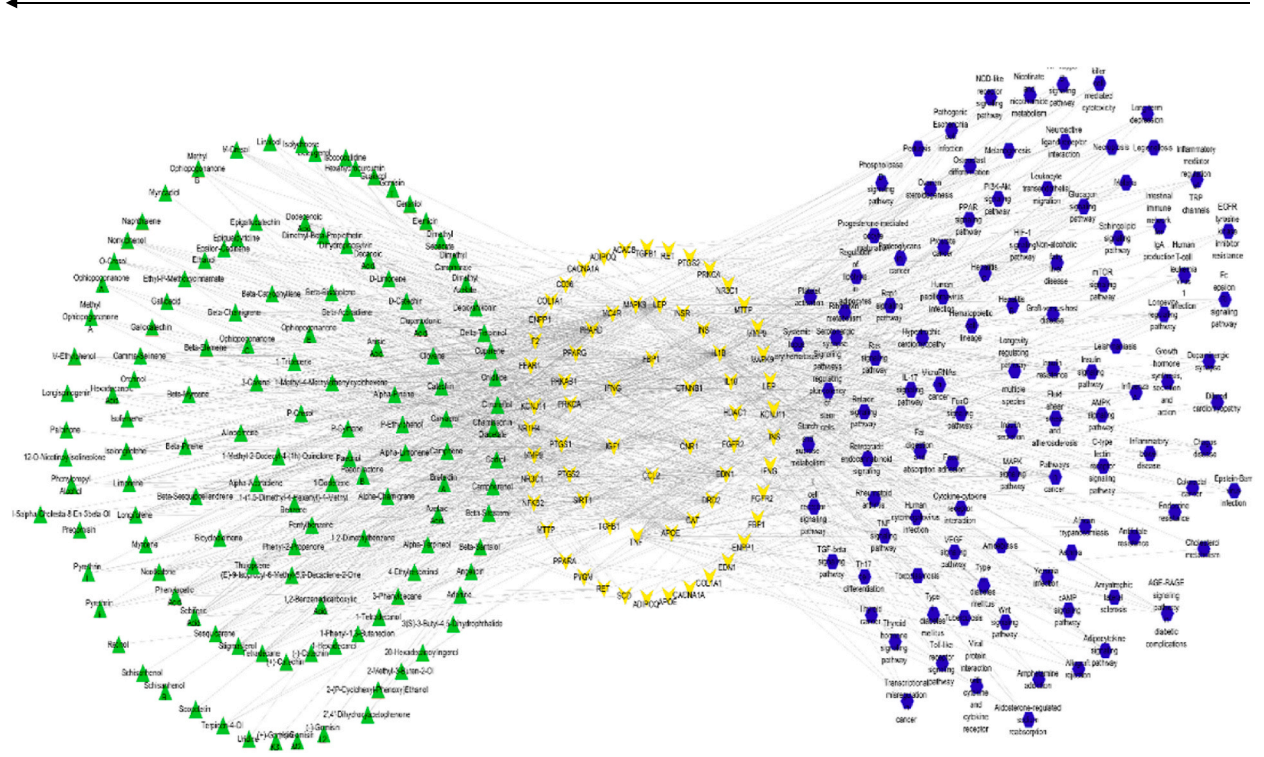


Fig. 15. Component-target-pathway network.

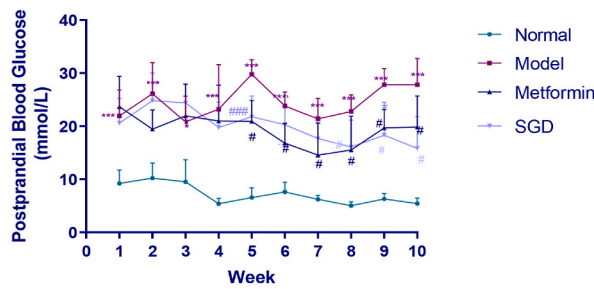


Fig. 16. Effect of SGD on Postprandial blood glucose level in *db/db* mice. Note: \* $p < 0.05$ , \*\* $p < 0.01$  all Groups vs Normal Group; # $p < 0.05$ , ## $p < 0.01$  all Groups vs Model Group.

residues, and extends the sugar chain with  $\alpha$ -1,4-glycosidic bonds, and is the rate-limiting enzyme of hepatic and muscle glycogen synthase. It has an important role in the regulation of glucose metabolism and the maintenance of glucose homeostasis.

Glycogen phosphorylase (GP) is able to catalyze the phospholysis of glycogen, which causes the glycogen molecules to break  $\alpha$ -1,4-glycosidic bonds one by one from the non-reducing end to remove the glucosyl group and release glucose 1-phosphate until it is near the first four glucosyl groups of  $\alpha$ -1,6-glycosidic bond branching point of glycogen molecule. PYGL, a subtype of GP, is mainly present in the liver and is the rate-limiting enzyme in glycogen metabolism, playing a role in maintaining blood glucose balance.

The experimental results showed that the liver glycogen content of *db/db* mice in the model group was significantly reduced compared with that in the normal control group. Besides, the GCK and GS contents were reduced, and the PYGL and G-6-Pase contents were significantly increased, which blocked the synthesis and decomposition of glycogen and caused the imbalance of liver glycogen metabolism. Compared with the model group, the liver glycogen contents in the metformin and SGD treatment groups were significantly increased, and several metabolic enzymes were regulated to restore the balance, indicating the effect and mechanism of SGD in regulating liver glycogen metabolism, as well as its effect in the treatment of type 2 diabetes mellitus.

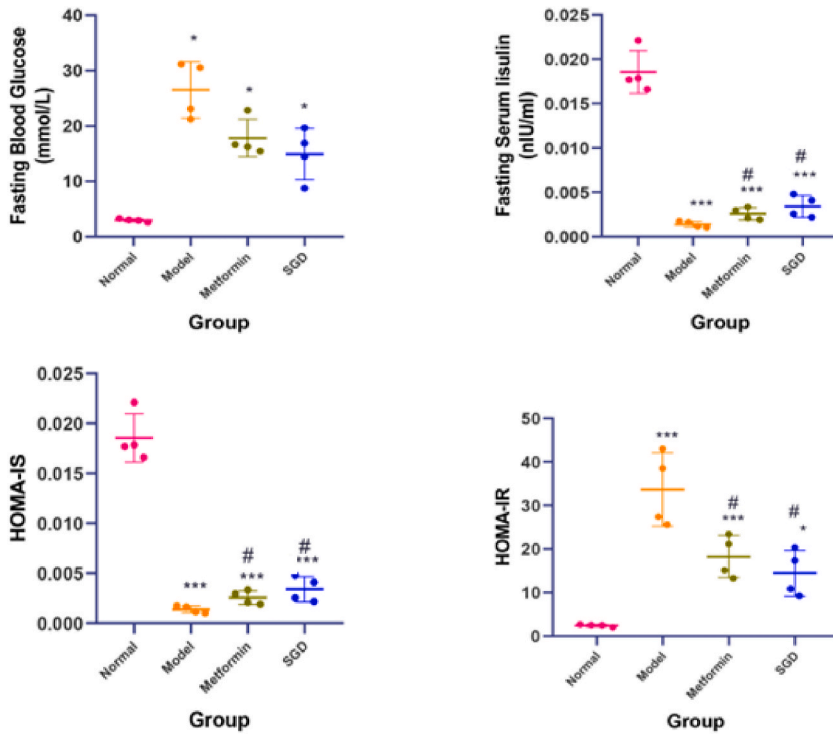


Fig. 17. Effect of SGD on FBG, FSIN, HOMA-IS and HOMA-IR levels in *db/db* mice. Note: \* $p < 0.05$ , \*\*\* $p < 0.01$ , all Groups vs Normal Group; # $p < 0.05$ , all Groups vs Model Group.

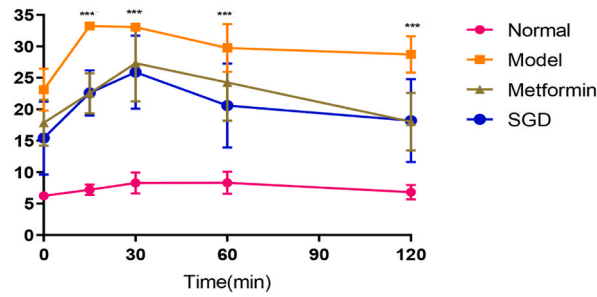


Fig. 18. Effect of SGD on IPGTT level in *db/db* mice. Note: \*\*\* $p < 0.01$  all Groups vs Normal Group.

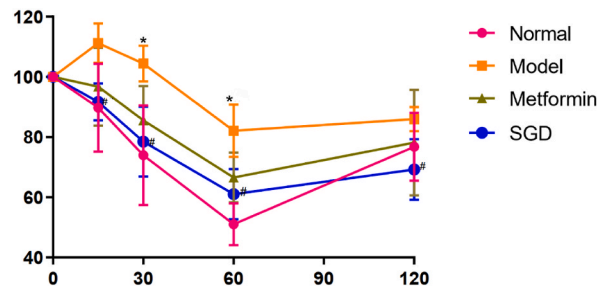
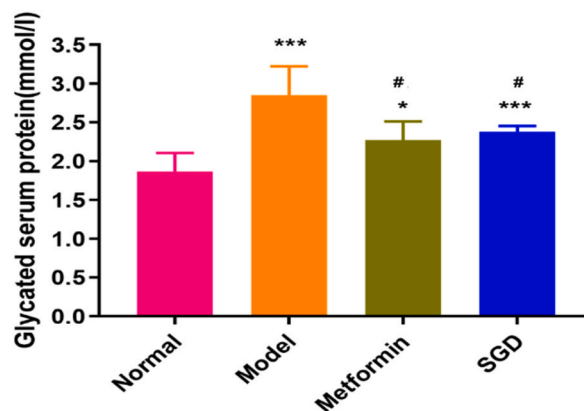


Fig. 19. Effect of SGD on IPITT level in *db/db* mice. Note: \* $p < 0.05$  all Groups vs Normal Group; # $p < 0.05$  all Groups vs Model Group.



**Fig. 20.** Effect of SGD on GSP level in *db/db* mice. Note: \* $p < 0.05$ , \*\*\* $p < 0.01$  all Groups vs Normal Group; # $p < 0.05$  all Groups vs Model Group.

**Table 5**

Effect of SGD on GS, Hepatic Glycogen GCK, PYGL and G-6-P levels in *db/db* mice.

	GS (mU/mg)	Hepatic glycogen (mg/g)	GCK (ng/mg)	PYGL (ng/mg)
Normal	42.21 ± 3.54	0.49 ± 0.02	211.55 ± 16.13	113.37 ± 6.21
Model	20.63 ± 1.51***	0.25 ± 0.04***	101.48 ± 8.63***	201.14 ± 10.96***
Metformin	38.31 ± 2.24###	0.41 ± 0.04*###	180.91 ± 16.25*###	125.65 ± 9.21
SGD	34.21 ± 2.33*###	0.52 ± 0.06###	208.74 ± 16.33*###	117.36 ± 7.38
				G-6-P (mU/mg)
Normal				114.93 ± 8.21
Model				208.88 ± 14.31***
Metformin				141.65 ± 9.06
SGD				132.39 ± 7.23

Note: \* $p < 0.05$ , \*\*\* $p < 0.01$  all Groups vs Normal Group; ### $p < 0.01$  all Groups vs Model Group;  $p < 0.05$  SGD Group vs Metformin Group.

**Table 6**

Effect of SGD on CAT, GSH-Px, MDA, T-SOD levels in *db/db* mice.

	CAT (U/mL)	T-SOD (U/mL)	GSH-Px (U/mL)	MDA (mmol/MI)
Normal	3.73 ± 0.35	119.38 ± 4.96	418.1 ± 3.41	4.32 ± 0.16
Model	1.5 ± 0.29***	97.39 ± 4.54*	186.94 ± 19.66***	8.82 ± 1.01***
Metformin	2.36 ± 0.26***#	123.86 ± 9.22*	367.58 ± 34.11*###	5.12 ± 0.61###
SGD	3.17 ± 0.17*###	140.29 ± 3.08***###	368.84 ± 15.71***###	4.82 ± 0.88###

Note: \* $p < 0.05$ , \*\*\* $p < 0.01$  all Groups vs Normal Group; # $p < 0.05$ , ### $p < 0.01$  all Groups vs Model Group;  $p < 0.05$ ,  $p < 0.01$  SGD Group vs Metformin Group.

**Table 7**

Effect of SGD on HDL-C, LDL-C, TC, and TG levels in *db/db* mice.

	HDL-C (mmol/L)	LDL-C (mmol/L)	TC (mmol/L)	TG (mmol/L)
Normal	2.1821 ± 0.09344	0.3924 ± 0.01478	2.5317 ± 0.2199	0.2798 ± 0.06591
Model	2.9821 ± 0.4310*	0.5898 ± 0.04190***	5.3195 ± 0.1493***	0.6157 ± 0.08255***
Metformin	3.7329 ± 0.2830***#	0.3385 ± 0.0770*###	4.4542 ± 0.4451***###	0.4196 ± 0.05679*#
SGD	3.5674 ± 0.5634***	0.3775 ± 0.03427###	4.4423 ± 0.3079***#	0.4309 ± 0.07571*#

Note: \* $p < 0.05$ , \*\*\* $p < 0.01$  all Groups vs Normal Group; # $p < 0.05$ , ### $p < 0.01$  all Groups vs Model Group.

#### 4.10. H.E. Staining of liver tissue in *db/db* mice

Many studies have shown that lipid accumulation in liver tissue is associated with type 2 diabetes, and since the liver is a major target organ for insulin action, it is an important site for glucolipid metabolism in the body. Under the stimulation of long-term fat and sugar intake, the metabolic function of the liver will be altered and its morphological structure will be changed.

The experimental results showed that the hepatocytes in the normal control group had regular morphology, with the nucleus located in the center of the cell, normal cell morphology, regular arrangement, intact and clear tissue structure, and no obvious

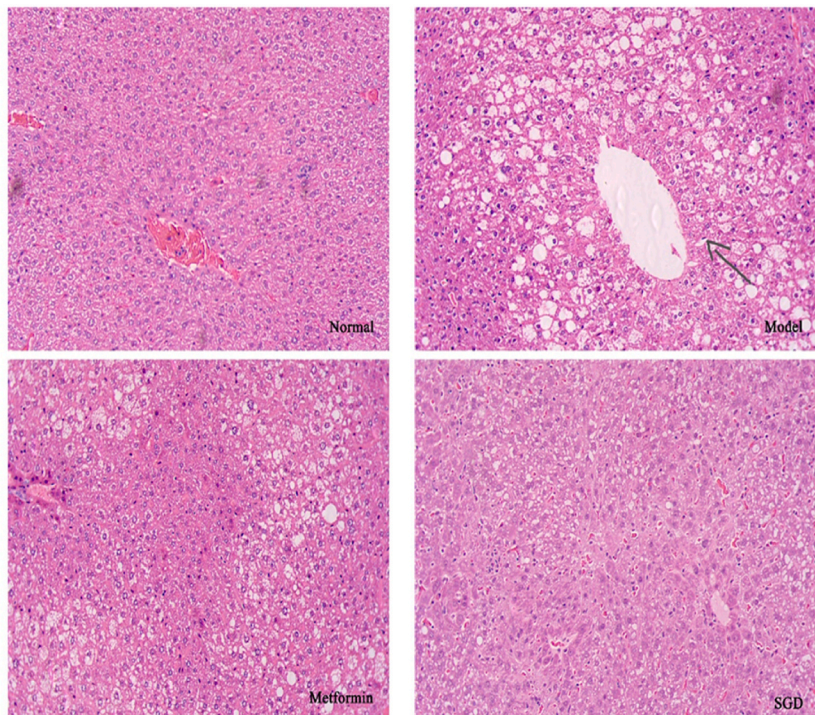


**Fig. 21.** H.E. staining of liver tissue in db/db mice.

pathological changes. In the model control group, a large number of hepatocytes showed swelling, disorganized and irregularly arranged; in the metformin group, hepatocytes showed swelling and necrosis, and disorganized cell arrangement; while in the SGD group, the morphology, arrangement and histological structure of hepatocytes were normal, with no obvious pathological changes.

#### 4.11. Protein expression of ACC, AMPK, FOXO1, AKT, p-AKT in db/db mice

AMPK signaling pathway is a key pathway for SGD treatment of T2DM. AMPK (Adenosine 5'-monophosphate (AMP)-activated protein kinase) is a key molecule for energy regulation, a cellular energy sensor and a homeostatic factor for regulating metabolism, and AMPK Activation of AMPK increases glucose utilization in adipose tissue, enhances fatty acid oxidation, hepatic glycogen conversion, and glucose uptake by skeletal muscle, and improves insulin resistance and insulin receptor sensitivity to maintain glucose homeostasis, which are key to the treatment of T2DM and related metabolic diseases [54].

PI3K/AKT signaling pathway is also a key pathway in SGD for the treatment of T2DM. Dysregulation of PI3K/Akt signaling pathway is seen in many human diseases, including cancer, diabetes, cardiovascular diseases and neurological diseases. In insulin effector tissues, the glucose In insulin effector tissues, the metabolic pathway of glucose is mainly through signaling pathways such as PI3K/Akt, and one of the target organs of insulin is the liver [55].

SGD inhibits T2DM-induced lipid accumulation by regulating the expression of related genes and proteins such as p-ACC, FAS and SREBP-1 (a downstream target of AMPK). SREBP-1 inhibits PI3K/AKT pathway by interfering with FOXO1 and decreases IRS-2 levels, thereby decreasing glycogen synthesis and causing insulin resistance [56].

Acetyl coenzyme A carboxylase (ACC) is the rate-limiting enzyme of fatty acid metabolism and plays an important role in the metabolism of fatty acids. AMPK induces the transfer of glucose transporter protein 4 (GLUT-4) to the plasma membrane and promotes glucose uptake in peripheral tissues by phosphorylating transcription factors [57].

Above all, the experimental results demonstrated that the levels of p-Akt, AMPK and ACC were significantly decreased and the levels of FOXO-1 were significantly increased in diabetic mice, while the administration of metformin and SGD could effectively increase the levels of phosphorylated Akt, AMPK and ACC, and decrease the levels of FOXO-1. The results showed that SGD can affect lipid and glucose metabolism by affecting AMPK/Akt pathway, and thus effectively relieve the symptoms of diabetes.

#### 4.12. Conclusion

The study indicated that SGD might improve insulin resistance and glucose metabolism in T2DM mice by activating the AMPK/Akt signaling pathway, which provided the foundation for further development of SGD as a new preparation for the prevention and treatment of T2DM. The results of this study are limited by the small sample size and the failure to conduct clinical trials with human samples. Therefore, multi-center and large sample size animal studies should be continued in the future to pave the way for future

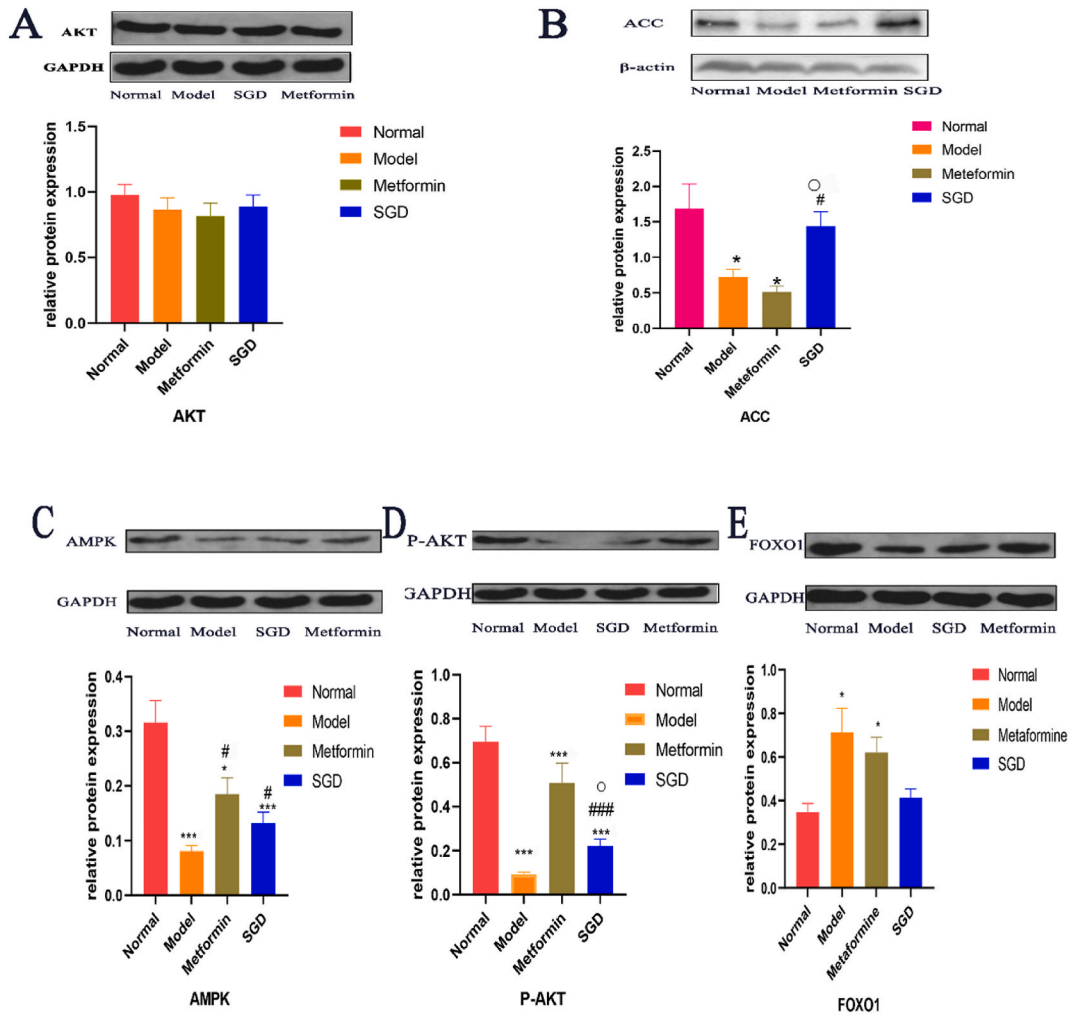


**Fig. 22.** The protein expression of the AMPK/Akt signaling pathway in the livers of db/db mice (A) The protein expression of AKT. (B) The protein expression of ACC. (C) The protein expression of AMPK. (D) The protein expression of p-Akt (E) the protein expression of FOXO1. Note: \* $p < 0.05$ , \*\*\* $p < 0.01$  all Groups vs Normal Group; # $p < 0.05$ , ### $p < 0.01$  all Groups vs Model Group;  $p < 0.05$  SGD Group vs Metformin Group.

human clinical trials.

**Author contribution statement**

Yunzhong Chen: Conceived and designed the experiments; Analyzed and interpreted the data; Contributed reagents, materials, analysis tools or data.

Yu cai: Conceived and designed the experiments; Analyzed and interpreted the data; Contributed reagents, materials, analysis tools or data; Wrote the paper.

SiMin Liu: Analyzed and interpreted the data; Contributed reagents, materials, analysis tools or data; Wrote the paper.

Zhiwei Rao; chunchao yan: Analyzed and interpreted the data; Contributed reagents, materials, analysis tools or data.

Fei Zeng; Qichang Xing: Performed the experiments; Analyzed and interpreted the data; Contributed reagents, materials, analysis tools or data.

**Data availability statement**

Data will be made available on request.

**Funding**

This research was funded by Natural Science Foundation of Hubei Province (2020CFB868).

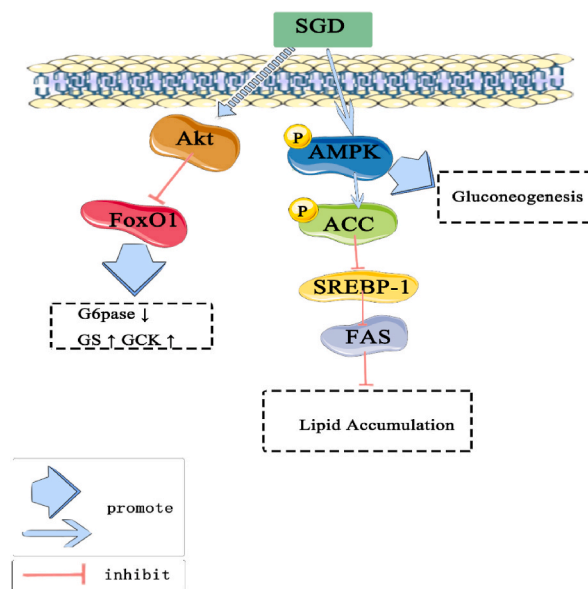


**Fig. 23.** Hypothetical molecular mechanism diagram: AMPK/Akt signaling pathway is involved in SGD-induced increase in lipid metabolism and gluconeogenesis, leading to increased GCK and GS levels.

### Declaration of competing interest

The authors declare that they have no known competing financial interests or personal relationships that could have appeared to influence the work reported in this paper

### Acknowledgement

We thank Mr. Min Zeng contributed for the Network pharmacology analysis in SGD of the manuscript.

### References

- [1] H Sun, P Saeedi, S Karuranga, et al., IDF Diabetes Atlas: Global, regional and country-level diabetes prevalence estimates for 2021 and projections for 2045, *Diabetes research and clinical practice* 183 (2022) 109119, <https://doi.org/10.1016/j.diabres.2021.109119>.
- [2] Gang Yang, Fangfang Su, Min Chen, Origins and prospects of medicinal food homologation, *China Mod. Tradit. Chin. Med.* 23 (11) (2021) 1851–1856, <https://doi.org/10.13313/j.issn.1673-4890.20211102004>.
- [3] Liujiao Huang, Yunzhong Chen, Li Jia Geng, Li Jageng's experience of using mulberry gourd drink in the treatment of diabetes mellitus, *Hubei J. Tradit. Chin. Med.* 38 (1) (2016) 32–33.
- [4] Ying Wang, Yu Cai, Zhi Fei, et al., Screening of effective parts for the hypoglycemic effect of mulberry gourd drink, *J. Hubei Univ. Chin. Med.* 18 (3) (2016) 50–53.
- [5] Qichang Xing, Ying Wang, Zhi Fei, et al., Investigation of the hypoglycemic effect of mulberry gourd drink on type 2 diabetic rats and preliminary investigation of the mechanism, *Shizhen Guoji Guomao* 27 (9) (2016) 2101–2103.
- [6] Yu Cai, Study on the Effect of Mulberry Gourd Drink Intervention in Type 2 Diabetic Rats and its PI3K/Akt Signaling Pathway Mechanism, Hubei University of Traditional Chinese Medicine, 2018.
- [7] Yu Cai, Ying Wang, Zhi Fei, Xing Qi-Chang, Chen Yun-Zhong, The effect of Sangguo drink extract on insulin resistance through the PI3K/AKT signaling pathway, *Evid. base Compl. Alternative Med. : eCAM* 2018 (2018).
- [8] Qian Zhang, Lihua Zhang, Chemical composition and progress of development and utilization of mulberry leaves, *Hubei Agric. Sci.* 59 (15) (2020) 16–19.
- [9] Xiaotian Zhou, Feijun Luo, Progress in the study of functional components and bioactivities of bitter melon, *Mod. Food* (10) (2020) 66–71.
- [10] Shuxin Li, Research progress on the chemical composition and pharmacological effects of Pueraria lobata, *Liaoning Chem. Ind.* 49 (11) (2020) 1412–1413.
- [11] Mengyu Chen, Wei Liu, Guixin Zhang, et al., Progress in the study of chemical composition and pharmacological activity of yam, *J. Tradit. Chin. Med.* 48 (2) (2020) 62–66.
- [12] N. Asano, R.J. Nash, R.J. Molyneux, et al., Sugar-mimic glycosidase inhibitors: natural occurrence, biological activity and prospects for therapeutic application, *Tetrahedron: Asymmetry* 11 (8) (2000) 1645–1680.
- [13] Lingyuan Xu, Li Rong, Tao Liang, et al., Study on the reversal of streptozotocin-induced pancreatic injury in diabetic mice by total flavonoids of Pueraria lobata, *Chinese J. Exp. Formul.* 19 (8) (2013) 231–234.
- [14] Chunyu Ma, Hongyu Yu, Huijiao Wang, et al., Study on the mechanism of hypoglycemic effect of total saponin of bitter melon on type 2 diabetic rats, *Tianjin Med.* 42 (4) (2014) 321–324.
- [15] Wenhui Xing, Jinli Hou, Hongpeng Han, et al., Effects of yam polysaccharides on blood glucose and antioxidant capacity in type I diabetic mice, *Food Res. Dev.* 35 (17) (2014) 107–110.
- [16] Rui Jin, Yinxiang Cheng, Fengmei Han, et al., Effects of yam polysaccharide on glycemic lipid and hepatic and renal oxidative stress in type I diabetic rats, *J. Hubei Univ. (Nat. Sci. Ed.)* 38 (4) (2016) 298–302.
- [17] Zhi Fei, Qichang Xing, Ying Wang, et al., Effects of Fructus yamensis polysaccharide on glucolipid metabolism and oxidative stress in type 2 diabetic rats, *Food Sci.* 38 (5) (2017) 262–266.



- [18] Yu Cai, Zhi Fei, Chen Yun Zhong, et al., Comparison of the antidiabetic effects of crude polysaccharides from Tiebang/Foiji yam, *Mod. Food Sci. Technol.* 38 (4) (2022) 10–18+215.
- [19] Yanqiong Zhang, Li Zu, Some advances in modern research on network pharmacology and Chinese medicine, *Chin. J. Pharmacol. Toxicol.* 29 (6) (2015) 883–892.
- [20] X. Wang, C. Pan, J. Gong, X. Liu, H. Li, Enhancing the enrichment of pharmacophore-based target prediction for the polypharmacological profiles of drugs, *J. Chem. Inf. Model.* 56 (6) (2016) 1175–1183.
- [21] H.Y. Fang, H.W. Zeng, L.M. Lin, et al., A network-based method for mechanistic investigation of Shexiang Baoxin Pill's treatment of cardiovascular diseases, *Sci. Rep.* 7 (2017), 43632.
- [22] J. Ru, P. Li, J. Wang, et al., TCMSP: a database of systems pharmacology for drug discovery from herbal medicines, *J. Cheminf.* 6 (2014) 13.
- [23] Lin Huang, Duoli Xie, Yiran Yu, Huanlong Liu, Yan Shi, Tieliu Shi, Chengping Wen, TCMID 2.0: a comprehensive resource for TCM, *Nucleic Acids Res.* 46 (D1) (2018).
- [24] Baiqing Li, Chunfeng Ma, Xiaoyong Zhao, Zhigang Hu, Tengfei Du, Xuanming Xu, Zhonghua Wang, Jianping Lin, YaTCM: yet another traditional Chinese medicine database for drug discovery, *Comput. Struct. Biotechnol. J.* 16 (2018).
- [25] Chagas Caroline Manto, Sara Moss, Alisaraie Laleh, Drug metabolites and their effects on the development of adverse reactions: revisiting Lipinski's Rule of Five, *Int. J. Pharm.* 549 (1–2) (2018).
- [26] Baiqing Li, Chunfeng Ma, Xiaoyong Zhao, et al., YaTCM: yet another traditional Chinese medicine database for drug discovery, *Comput. Struct. Biotechnol. J.* 16 (600–610) (2018).
- [27] H. Yang, W. Zhang, C. Huang, et al., A novel systems pharmacology model for herbal medicine injection: a case using Reduning injection, *BMC Compl. Alternative Med.* 14 (2014) 430.
- [28] X. Xu, W. Zhang, C. Huang, et al., A novel chemometric method for the prediction of human oral bioavailability, *Int. J. Mol. Sci.* 13 (6) (2012) 6964–6982.
- [29] C.A. Lipinski, F. Lombardo, B.W. Dominy, P.J. Feeney, Experimental and computational approaches to estimate solubility and permeability in drug discovery and development settings, *Adv. Drug Deliv. Rev.* 46 (1–3) (2001) 3–26.
- [30] Z.J. Yao, J. Dong, Y.J. Che, et al., TargetNet: a web service for predicting potential drug-target interaction profiling via multi-target SAR models, *J. Comput. Aided Mol. Des.* 30 (5) (2016) 413–424.
- [31] X. Wang, Y. Shen, S. Wang, et al., PharmMapper 2017 update: a web server for potential drug target identification with a comprehensive target pharmacophore database, *Nucleic Acids Res.* 45 (W1) (2017) W356–W360.
- [32] A. Daina, O. Michielin, V. Zoete, SwissTargetPrediction: updated data and new features for efficient prediction of protein targets of small molecules, *Nucleic Acids Res.* 47 (W1) (2019) W357–W364.
- [33] J. Piñero, J.M. Ramírez-Angueta, J. Saüch-Pitarch, et al., The DisGeNET knowledge platform for disease genomics: 2019 update, *Nucleic Acids Res.* 48 (D1) (2020) D845–D855.
- [34] G. Stelzer, N. Rosen, I. Plaschkes, et al., The GeneCards suite: from gene data mining to disease genome Sequence analyses, *Curr. Protoc. Bioinf.* 54 (2016) 1, 30.1-1.30.33.
- [35] P. Shannon, A. Markiel, O. Ozier, et al., Cytoscape: a software environment for integrated models of biomolecular interaction networks, *Genome Res.* 13 (11) (2003) 2498–2504.
- [36] Y. Zhou, B. Zhou, L. Pache, et al., Metascape provides a biologist-oriented resource for the analysis of systems-level datasets, *Nat. Commun.* 10 (1) (2019) 1523.
- [37] Ravi Naik, Dipesh S. Harmalkar, Xuezheng Xu, et al., Bioactive benzofuran derivatives: Moracins AeZ in medicinal chemistry, *Eur. J. Med. Chem.* 90 (2015) 379–393.
- [38] Changyong Xue, Yinghua Liu, Rongxin Zhang, et al., Effects of flavonoids from *Morus alba* L. on activity of alpha-glucosidase, *Chinese Journal of Tissue Engineering Research* 11 (21) (2007) 4191–4193, <https://doi.org/10.3321/j.issn:1673-8225.2007.21.053>.
- [39] Mingli. Luo, Relationship between the Hypoglycemic Effect of Active Parts of *Morus Alba* and JNK Signaling Pathway, *Guangzhou University of Chinese Medicine* (2013).
- [40] Q. Liu, F.G. Zhang, W. Song, Y.L. Yang, J.F. Liu, P. Li, B.L. Liu, W. Qi, Ginsenoside Rg1 inhibits glucagon-induced hepatic gluconeogenesis through Akt-FoxO1 interaction, *Arch. Med. Res.* 49 (2018) 314–322.
- [41] H.U. Chowdhury, M. Adnan, K.K. Oh, et al., Decrypting molecular mechanism insight of *Phyllanthus emblica* L. fruit in the treatment of type 2 diabetes mellitus by network pharmacology, *Phytomedicine* 1 (4) (2021), 100144.
- [42] K.K. Oh, M. Adnan, D.H. Cho, Network pharmacology of bioactives from *Sorghum bicolor* with targets related to diabetes mellitus, *PLoS One* 15 (12) (2021), e0240873.
- [43] K.P. Hummel, M.M. Dickie, D.L. Coleman, Diabetes, a new mutation in the mouse, *Science* 153 (3740) (1966) 1127–1131.
- [44] S.H. Kwak, K.S. Park, Recent progress in genetic and epigenetic research on type 2 diabetes, *Exp. Mol. Med.* 48 (3) (2016), e220.
- [45] J.D. McGarry, Banting lecture 2001: dysregulation of fatty acid metabolism in the etiology of type 2 diabetes, *Diabetes* 51 (2002) 7–18.
- [46] W. März, M.E. Kleber, H. Scharnagl, T. Speer, S. Zewinger, A. Ritsch, K.G. Parhofer, A. von Eckardstein, U. Landmesser, U. Laufs, HDL cholesterol: reappraisal of its clinical relevance, *Clin. Res. Cardiol.* 106 (9) (2017 Sep) 663–675.
- [47] I. Demir, N. Kiyamaz, B. Gudu, et al., Study of the neuroprotective effect of ginseng on superoxide dismutase (SOD) and glutathione peroxidase (GSH-Px) levels in experimental diffuse head trauma, *Acta Neurochir. (Wien)* 155 (5) (2013) 913–922.
- [48] Manhua Zuo, Jun Tang, Assessment of serum oxidative stress, angiogenic indicators and peripheral blood T-cell levels in elderly patients with diabetic nephropathy at different stages, *Chin. J. Mod. Med.* 25 (31) (2015) 74–77.
- [49] D. Del Rio, A.J. Stewart, N. Pellegrini, A review of recent studies on malondialdehyde as toxic molecule and biological marker of oxidative stress, *Nutr. Metabol. Cardiovasc. Dis.* 15 (4) (2005) 316–328.
- [50] X. Zou, Z. Feng, Y. Li, et al., Stimulation of GSH Synthesis to prevent oxidative stress-induced apoptosis by hydroxytyrosol in human retinal pigment epithelial cells: Activation of Nrf2 and JNK-P62/SQSTM1 Pathways, *J. Nutr. Biochem.* 23 (8) (2012) 994–1006.
- [51] A. Ceriello, R. Testa, Antioxidant anti-inflammatory treatment in type 2 diabetes, *Diabetes Care* 32 (Suppl 2) (2009) 232–236.
- [52] R.J. Johnson, T. Nakagawa, L.G. Sanchez-Lozada, et al., Sugar, uric acid, and the etiology of diabetes and obesity, *Diabetes* 62 (10) (2013) 3307–3315.
- [53] D. Zelent, H. Najafi, S. Odili, et al., Glucokinase and glucose homeostasis: proven concepts and new ideas, *Biochem. Soc. Trans.* 33 (Pt 1) (2005) 306–310.
- [54] Sheng Qin, Yanxiu Wang, Jiabao Chen, et al., Research progress on the hypoglycemic effect of traditional Chinese medicine based on AMPK signaling pathway, *Chin. Pharm.* 20 (12) (2017) 2225–2228.
- [55] Yu-Jing Chi, Jing Li, You-Fei Guan, et al., PI3K/Akt signaling Axis in regulation of glucose homeostasis, *Chin. J. Biochem. Mol. Biol.* 26 (10) (2010) 879–885.
- [56] D.J. Fan, G.Q. Xu, Advances in the study of solid alcohol regulatory element binding proteins and lipid metabolism, *Int. J. Intern. Med.* (3) (2007) 152–154+173.
- [57] Z.J. Lin, B. Zhang, S.Q. Liu, Advances in AMPK-ACC signaling pathway and related metabolic diseases, *Chin. J. Diabetes* 21 (5) (2013) 474–477.